


# Thymosin $\alpha$ 1 represents a potential potent single-molecule-based therapy for cystic fibrosis

Luigina Romani<sup>1</sup>, Vasilis Oikonomou<sup>1</sup>, Silvia Moretti<sup>1</sup>, Rossana G Iannitti<sup>1</sup>, Maria Cristina D'Adamo<sup>2</sup>, Valeria R Villella<sup>3</sup>, Marilena Pariano<sup>1</sup>, Luigi Sforna<sup>1</sup>, Monica Borghi<sup>1</sup>, Marina M Bellet<sup>1</sup>, Francesca Fallarino<sup>1</sup>, Maria Teresa Pallotta<sup>1</sup>, Giuseppe Servillo<sup>1</sup>, Eleonora Ferrari<sup>3</sup>, Paolo Puccetti<sup>1</sup>, Guido Kroemer<sup>4-7</sup>, Mauro Pessia<sup>1,2</sup>, Luigi Mairuri<sup>3,8</sup>, Allan L Goldstein<sup>9</sup> & Enrico Garaci<sup>10,11</sup> 

**Q4** Cystic fibrosis (CF) is caused by mutations in the gene encoding the cystic fibrosis transmembrane conductance regulator (CFTR) that compromise its chloride channel activity. The most common mutation, p.Phe508del, results in the production of a misfolded CFTR protein, which has residual channel activity but is prematurely degraded. Because of the inherent complexity of the pathogenetic mechanisms involved in CF, which include impaired chloride permeability and persistent lung inflammation, a multidrug approach is required for efficacious CF therapy. To date, no individual drug with pleiotropic beneficial effects is available for CF. **Q5** Here we report on the ability of thymosin alpha 1 (T $\alpha$ 1)—a naturally occurring polypeptide with an excellent safety profile in the clinic when used as an adjuvant or an immunotherapeutic agent—to rectify the multiple tissue defects in mice with CF as well as in cells from subjects with the p.Phe508del mutation. T $\alpha$ 1 displayed two combined properties that favorably opposed CF symptomatology: it reduced inflammation and increased CFTR maturation, stability and activity. **Q6** By virtue of this two-pronged action, T $\alpha$ 1 has strong potential to be an efficacious single-molecule-based therapeutic agent for CF.

**Q19** **Q7** CF is an autosomal recessive disorder caused by different mutations in the CF-associated gene encoding the CFTR protein (see URLs<sup>1</sup>). Presently, various pharmacological agents that target specific classes of CFTR mutations to address the basic defects in CF improve CFTR function and alter the disease process<sup>2</sup>. The p.Phe508del mutation in the first nucleotide-binding domain, which is the most common mutation among individuals with CF, results in the production of a misfolded protein with residual activity that is degraded by the ubiquitin–proteasome system during biogenesis<sup>2,3</sup>. Corrector drugs rescue trafficking of p.Phe508del-CFTR to the plasma membrane by directly targeting the mutant protein<sup>2-4</sup>. However, in spite of their high efficacy *in vitro*, CFTR correctors show modest clinical benefits in individuals with CF who harbor the p.Phe508del mutation, even when these correctors are combined with the CFTR potentiator ivacaftor<sup>5,6</sup>. **Q17** **Q8** Given the complex molecular and cellular defects that occur in CF, a multidrug approach is desirable to both rescue and stabilize p.Phe508del-CFTR *in vivo* and, hence, prevent the progressive decline of lung function in individuals with CF<sup>7</sup>. **Q18** Recently, general strategies aimed at improving the proteostasis network by means of proteostasis regulators have emerged as an alternative approach to promote p.Phe508del-CFTR plasma membrane targeting and stability<sup>8,9</sup>. Instead of directly targeting the mutant protein, proteostasis regulators

favor p.Phe508del-CFTR rescue and stability by altering signaling pathways and checkpoints in cellular proteostasis<sup>8-10</sup>.

Optimal CF treatments should not only rescue CFTR localization and functionality but also alleviate the associated hyperinflammatory pathology<sup>2,8</sup>. Rescuing chloride channel activity might be sufficient *per se* to reverse the inflammatory pathology in chronic CF lung disease<sup>11,12</sup>. However, the complexity of the p.Phe508del-CFTR molecular defect makes this task challenging. Irrespective of whether the inflammatory response is due to multiple, additive effects—including chronic infection—or is a primary outcome of CFTR dysfunction, a hyperinflammatory state in individuals with CF is associated, as a rule, with early and nonresolving activation of innate immunity, which impairs microbial clearance and promotes a self-sustaining condition of progressive lung damage<sup>13</sup>. The remarkable persistence of chronic lung infections in the face of intensive antibiotic therapy<sup>14</sup> and, likewise, the major side-effects of both corticosteroids<sup>15</sup> and non-steroidal anti-inflammatory drugs (NSAIDs), including inhibition of the CFTR chloride channel<sup>16</sup>, have revealed the need for therapeutic approaches aimed at activating early anti-inflammatory pathways to prevent, rather than correct, organ damage before patients become symptomatic. **Q10** Moreover, hyperinflammatory mucosal responses to either cell-autonomous or environmental (for example, bacterial) **Q11**

**Q2** <sup>1</sup>Department of Experimental Medicine, University of Perugia, Perugia, Italy. <sup>2</sup>Department of Physiology and Biochemistry, Faculty of Medicine and Surgery, University of Malta, Malta. <sup>3</sup>European Institute for Research in Cystic Fibrosis, Division of Genetics and Cell Biology, San Raffaele Scientific Institute, Milan, Italy. <sup>4</sup>Centre de Recherche des Cordeliers, INSERM U1138, Université Paris Descartes, Paris, France. <sup>5</sup>Metabolomics and Cell Biology Platforms, Institut Gustave Roussy, Villejuif, France. <sup>6</sup>Pôle de Biologie, Hôpital Européen Georges Pompidou, AP-HP, Paris, France. <sup>7</sup>Karolinska Institute, Department of Women's and Children's Health, Karolinska University Hospital, Stockholm, Sweden. <sup>8</sup>Department of Health Sciences, University of Piemonte Orientale, Novara, Italy. <sup>9</sup>Department of Biochemistry and Molecular Medicine, George Washington University, School of Medicine and Health Sciences, Washington, DC, USA. <sup>10</sup>University San Raffaele, Rome, Italy. <sup>11</sup>IRCCS San Raffaele, Rome, Italy. Correspondence should be addressed to L.R. (luigina.romani@unipg.it).

Received 4 August 2016; accepted 17 February 2017; published online XX XX 2017; doi:10.1038/nm.4305

stresses can further compromise cellular proteostasis, thus affecting CFTR trafficking and function in a feed-forward loop<sup>10</sup>. Therefore, the ideal anti-inflammatory drug in CF should be one that not only interrupts the vicious CF cycle that sustains inflammation but also generates favorable conditions for CFTR trafficking. To date, no single drug is available with such positive pleiotropic effects in individuals with CF.

T $\alpha$ 1 is a naturally occurring polypeptide of 28 amino acids<sup>17</sup> whose mechanism of action as an immune modulator presumably involves an ability to signal through innate immune receptors<sup>18</sup> that are activated by dynamic association with membrane phosphatidylserine<sup>19</sup>. T $\alpha$ 1 (Zadaxin) is used worldwide as an immunomodulator in viral infections, immunodeficiencies, malignancies and HIV/AIDS<sup>20</sup>. Owing to its ability to activate the tolerogenic pathway of tryptophan catabolism via the immunoregulatory enzyme indoleamine 2,3-dioxygenase 1 (IDO1)<sup>21</sup>, T $\alpha$ 1 specifically potentiates immune tolerance in the lung, often breaking the vicious circle that perpetuates chronic lung inflammation in response to a variety of infectious noxae<sup>18</sup>. This led us to hypothesize that administration of T $\alpha$ 1 could be beneficial in CF to alleviate early inflammation. Here we report that T $\alpha$ 1 is endowed with a unique property consisting of a dual ability to control inflammation and rectify the functional defects of p.Phe508del-CFTR.

## RESULTS

### T $\alpha$ 1 improves inflammation and immune tolerance in CF

Inflammation plays a critical role in lung disease development and progression in CF. IDO1, which is known to inhibit pathogenic T helper type 17 (T<sub>H</sub>17) cell activation and to initiate immune tolerance mechanisms in the lungs<sup>21</sup>, is defective in individuals with the p.Phe508del mutation in CFTR<sup>22</sup>. In accordance with an ability to induce IDO1 via Toll-like receptor 9 (TLR9) signaling<sup>18</sup>, T $\alpha$ 1 promoted TLR9 colocalization in lysosomes (Fig. 1a), where maturation and signaling of TLR9 occur in response to stimulatory CpG oligodeoxynucleotides (ODN)<sup>23</sup>. Concomitantly, T $\alpha$ 1 rescued defective IDO1 expression in an airway epithelial cell line (CFBE41o-) stably expressing p.Phe508del-CFTR<sup>24</sup> (Fig. 1b). In doing so, T $\alpha$ 1 reduced proinflammatory nuclear factor (NF)- $\kappa$ B activity in response to the TLR2 ligand MALP-2 (Fig. 1c,d) and promoted IRF3 phosphorylation and expression of the anti-inflammatory cytokine *IL10* (Fig. 1e), which are both known to contribute to immune tolerance in the lung<sup>18</sup>. T $\alpha$ 1 also rescued defective IDO1 expression when administered *in vivo* to C57BL/6 mice homozygous for a *Cftr* allele encoding p.Phe508del (*Cftr*<sup>F508del/F508del</sup> mice; hereafter referred to as *Cftr*<sup>F508del</sup> mice) infected with *Aspergillus fumigatus*, which colonizes CF airways and contributes to chronic lung disease<sup>25</sup>. Mice received T $\alpha$ 1 either intraperitoneally or intranasally (Supplementary Fig. 1a,b) soon after infection or in an established infection model (Supplementary Fig. 1c–e) daily for 6 d at 200  $\mu$ g per kg bodyweight, which is a dose previously shown to exert therapeutic activity in preclinical settings<sup>26</sup> and to approximate, on a weight-per-weight basis, T $\alpha$ 1 doses that can be safely administered to humans<sup>27</sup>. T $\alpha$ 1 restored IDO1 expression both basally and after infection (Fig. 1f and Supplementary Fig. 1a) and concomitantly reduced caspase-1 cleavage (Fig. 1g) and NLRP3 expression (insets of Fig. 1h), thus reducing inflammasome activity. At the same time, it reduced lung pathology in naive and infected mice (Fig. 1h and Supplementary Fig. 1d), fungal colonization (Fig. 1i and Supplementary Fig. 1c) and neutrophil infiltration (Fig. 1j and Supplementary Fig. 1b,e). Levels of the inflammatory cytokines tumor necrosis factor (TNF)- $\alpha$ , IL-1 $\beta$  and IL-17A were all reduced, and IL-10 levels, as well as those of IL-1Ra, were increased

by T $\alpha$ 1 (Fig. 1k and Supplementary Fig. 1b,e), which suggests that T $\alpha$ 1—via IDO1 induction—may also restrain pathogenic inflammasome activity in CF<sup>28</sup>. Similar results were obtained in *Cftr*<sup>+/-</sup> and *Cftr*<sup>-/-</sup> mice (Supplementary Fig. 2a–d), indicating that the anti-inflammatory activity of T $\alpha$ 1 occurs independently of CFTR expression and function. T $\alpha$ 1 also restrained inflammation and lung colonization in *Pseudomonas aeruginosa* infection (Supplementary Fig. 2e–g), indicating that it might favorably affect microbiology in the CF-infected lung.

A limited but significant increase in body weight was afforded by T $\alpha$ 1 treatment (Supplementary Fig. 3a), which prompted us to examine the effects of T $\alpha$ 1 on gut morphology in mutant mice, while also considering that loss-of-function mutations of *Cftr* cause a predominantly intestinal phenotype<sup>29</sup>. Similar to what was observed in the lung, T $\alpha$ 1 rescued IDO1 expression, tissue architecture, barrier function and cytokine balance in the small intestines of *Cftr*<sup>F508del</sup> mice (Supplementary Fig. 3b–e). This further suggested that T $\alpha$ 1, by influencing CF inflammation and microbiology, favorably alters the natural history of the disease.

### T $\alpha$ 1 improves the localization and stability of mutant CFTR

Infection and inflammation may produce secondary alterations in CFTR expression and function<sup>30</sup>. This might imply that efficient control of inflammation would improve CFTR functioning. Considering that IDO1 is a potent driver of autophagy<sup>31</sup> and that restoring disabled autophagy in CF will rescue CFTR function<sup>9,32</sup>, we interrogated whether T $\alpha$ 1 treatment would also affect CFTR functioning. We found that T $\alpha$ 1 favored trafficking of mature CFTR in CFBE41o- cells stably expressing p.Phe508del-CFTR. CFTR exit from the endoplasmic reticulum, passage through the Golgi and delivery of the mature form (band C) to the cell surface are accompanied by an increase in molecular weight (from 135–140 to 170–180 kDa) as a result of glycosylation. At a clinically attainable dose<sup>33</sup>, T $\alpha$ 1 increased cellular expression of mature p.Phe508del-CFTR (Fig. 2a, band C) by 10-fold  $\pm$  0.5-fold relative to vehicle-treated cells (Fig. 2b), reaching levels as high as 52  $\pm$  7% of control values. The effect was observed at 30 min and up to 24 h after treatment (Fig. 2a), was dose dependent (Fig. 2c) and was still somewhat detectable at 24 h after T $\alpha$ 1 removal (Fig. 2d).

Low-temperature treatment of airway cells harboring the p.Phe508del-CFTR mutation alleviates the processing defect of the mutant protein, enhancing its plasma membrane localization<sup>34</sup>. T $\alpha$ 1 increased plasma membrane localization of p.Phe508del-CFTR to the half-maximal value afforded by low-temperature incubation (Fig. 2e,f), as revealed by immunoblotting of purified plasma membrane fractions (FLOT-1<sup>+</sup>) with anti-CFTR antibody (Fig. 2g,h) and immunofluorescence staining (Fig. 2i). We found clear restriction of p.Phe508del-CFTR proteins around the nucleus in untreated CFBE41o- cells, in opposition to the mutated protein's migration to the plasma membrane after T $\alpha$ 1 treatment. This suggested that T $\alpha$ 1 increases the conformational stability of p.Phe508del-CFTR in the ER, thus allowing its exit from the ER and its trafficking to the cell surface. This was confirmed by the limited proteolysis assay, which measures resistance to proteolytic digestion of folded versus unfolded proteins<sup>35</sup>. T $\alpha$ 1 reduced the proteolytic digestion of p.Phe508del-CFTR (Fig. 2j).

As Rab GTPases modulate the intracellular trafficking of CFTR through the endosomal and recycling compartments<sup>36</sup>, we performed immunostaining of p.Phe508del-CFTR with markers of early (Rab5), late (Rab7) and recycling (Rab9) endosomes after T $\alpha$ 1 exposure. T $\alpha$ 1 reduced colocalization of mutant CFTR with Rab5 and Rab7, and it instead promoted colocalization with Rab9 (Fig. 2k), indicating that

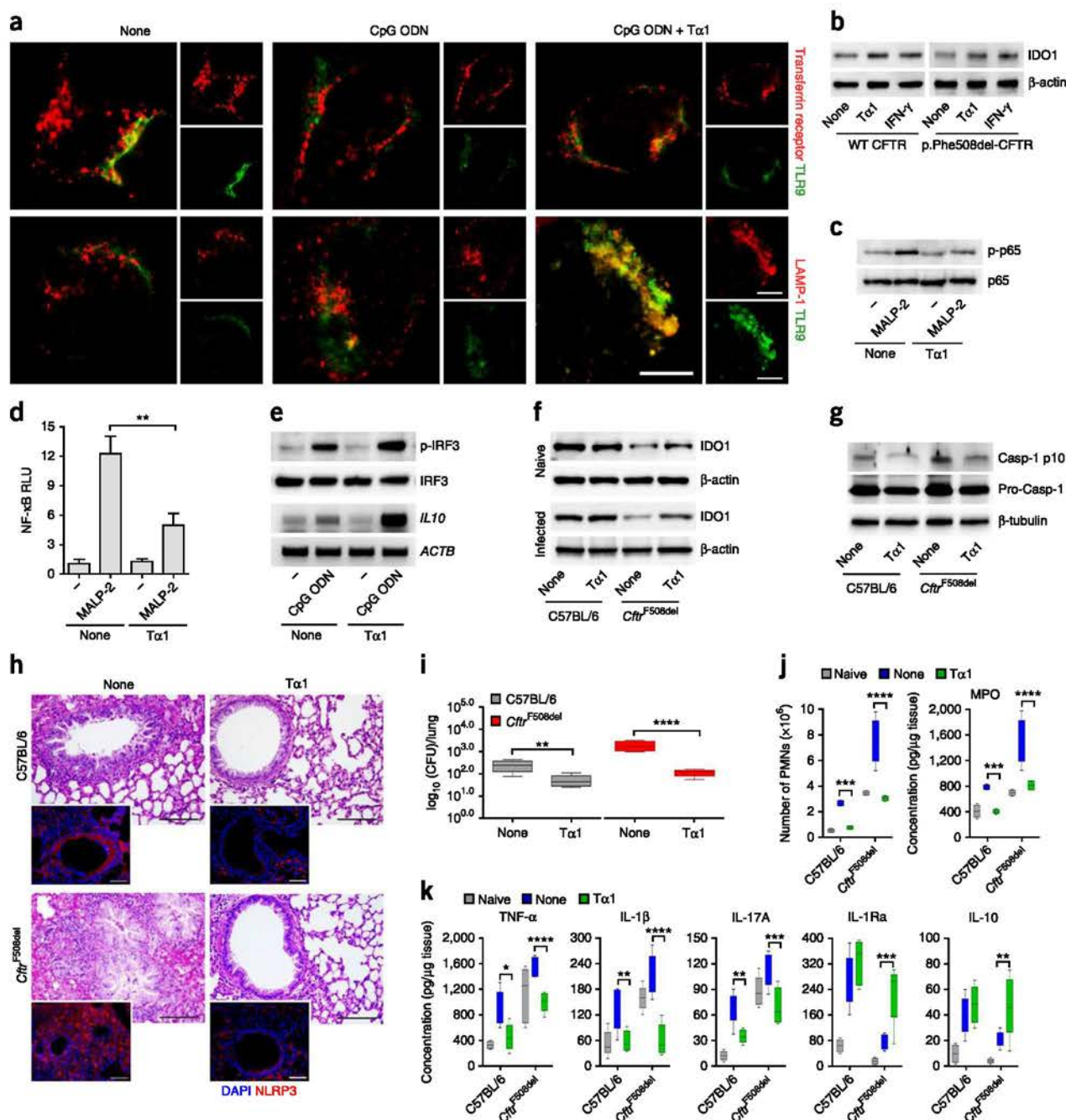
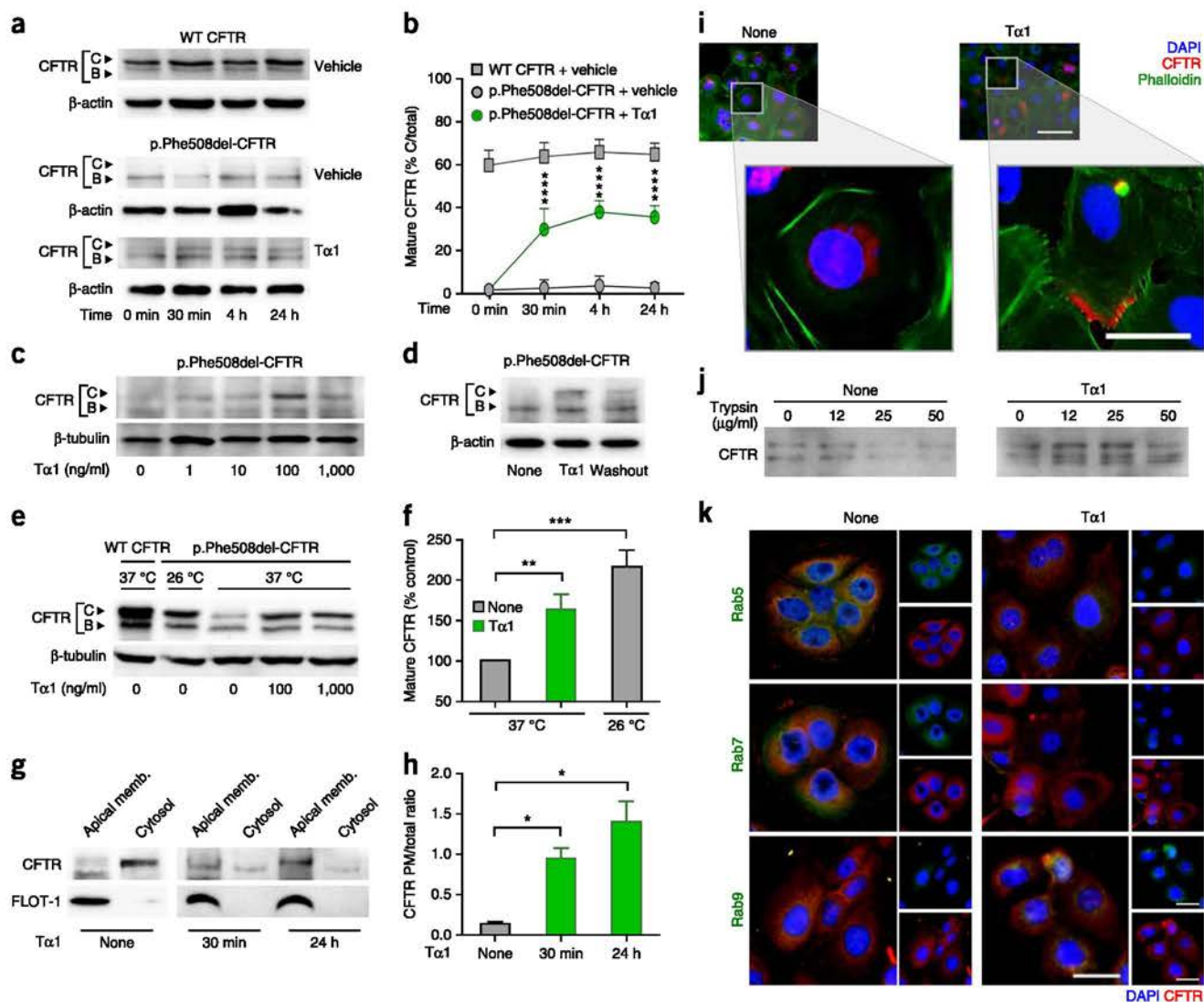


**Figure 1** Tα1 limits the inflammatory response in cystic fibrosis via IDO1. (a) Representative images ( $n = 5$  images per treatment) of TLR9 colocalization with transferrin receptor and LAMP-1 on endosomes in HEK293 cells transfected with human TLR9-GFP and stimulated with a suboptimal CpG ODN dose with or without 100 ng/ml Tα1. Scale bars, 100 μm. Shown are merged images of cells (single-channel FITC or TRITC images are on the right). See **Supplementary Figure 10** for colocalization coefficients. (b) CFBE41o- cells transfected with WT CFTR or p.Phe508del-CFTR were treated with Tα1 or 100 U/ml interferon (IFN)-γ as a positive control for 24 h at 37 °C. Shown are representative immunoblots ( $n = 3$ ) of IDO1 protein. (c) CFBE41o- cells transfected with p.Phe508del-CFTR and exposed to MALP-2 in the presence of Tα1 for 2 h. Representative immunoblots ( $n = 3$ ) of NF-κB/p65 (p65) and phosphorylated NF-κB/p65 (p-p65) are shown. (d) CFBE41o- cells were transfected with an NF-κB luciferase reporter plasmid and p.Phe508del-CFTR with MALP-2 exposure and Tα1 treatment. NF-κB relative luciferase units (RLU) are shown from  $n = 3$  replicates. (e) CFBE41o- cells were transfected with p.Phe508del-CFTR and exposed to CpG ODN in the presence of Tα1 for 2 h. Representative immunoblots ( $n = 3$ ) of IRF3 and phosphorylated IRF3 (p-IRF3) (top) and *IL10* gene expression ( $n = 3$ ) (bottom) are shown. (f-h) Control C57BL/6 and *Cfr*<sup>F508del</sup> mice were infected intranasally with live *A. fumigatus* conidia and treated with 200 μg per kg bodyweight Tα1 intraperitoneally for 6 d. Lungs were assessed for IDO1 protein (f) and caspase-1 cleavage (g) by immunoblotting and examined for histology (periodic acid-Schiff (PAS) staining) and immunofluorescence staining with NLRP3 antibody ( $n = 5$  images per mouse) (h). Scale bars, 100 μm. Immunoblotting and lung sections are representative of three independent experiments with  $n = 6$  mice per group. (i) Fungal growth ( $\log_{10}$  colony-forming units (CFU)). (j,k) Number of polymorphonuclear neutrophils (PMNs) in the bronchoalveolar lavage (BAL) and MPO (j) as well as cytokine (k) production in lung homogenates. Assays were performed 7 d after infection. Data (means  $\pm$  s.d.) are presented as box-and-whisker plots; bars represent maximal and minimal values. \* $P < 0.05$ , \*\* $P < 0.01$ , \*\*\* $P < 0.001$ , \*\*\*\* $P < 0.0001$ , two-way ANOVA with Tukey's post test. None, treatment with scrambled peptide; -, untreated cells.



**Q77** **Figure 2** Tα1 increases cell surface expression and stability of p.Phe508del-CFTR. **Q78** (a) Representative CFTR immunoblots ( $n = 3$ ) from CFBE41o- cells **Q79** transfected with WT CFTR or p.Phe508del-CFTR and treated with 100 ng/ml Tα1 or vehicle at various time points. Arrowheads indicate the B and C (mature) forms of CFTR. **Q80** (b) Percentage of band C to total (bands B + C) CFTR as quantified by densitometry for the cells in a. **Q81** (c–e) CFTR immunoblots from CFBE41o- cells transfected with p.Phe508del-CFTR and incubated with different doses of Tα1 (c), incubated with Tα1 for 24 h with or without a subsequent 12-h washout at 37 °C (d), and incubated with Tα1 for 24 h at 26 °C or 37 °C (e). The blots shown are each representative of  $n = 3$  experiments. **Q82** (f) Relative percentage of band C to total CFTR (expressed as the percentage of control). **Q83** (g) Representative immunoblots ( $n = 5$ ) of CFTR **Q84** and FLOT-1 for purified plasma membranes from CFBE41o- cells incubated with Tα1 at 37 °C. (h) Fold increase in CFTR at the plasma membrane (PM) relative to total CFTR. (i) Immunofluorescence staining of CFTR ( $n = 5$  images per treatment) in CFBE41o- cells treated with Tα1 for 24 h. **Q85** (j) Immunoblots of CFTR in CFBE41o- cells treated with Tα1 for 24 h at 37 °C and exposed to trypsin. (k) Immunostaining of CFTR with Rab5, Rab7, or Rab9 ( $n = 5$  images per treatment) in CFBE41o- cells treated with Tα1 at 37 °C for 2 h. Shown are merged images of cells. See **Supplementary Figure 10** for colocalization coefficients. In i and k, scale bars, 100 μm. Data are presented as means ± s.d. \* $P < 0.05$ , \*\* $P < 0.01$ , \*\*\* $P < 0.001$ , \*\*\*\* $P < 0.0001$ , two-way or one-way ANOVA with Tukey's post test.

Tα1 reduces endocytic recycling through the early endosomes, prevents movement to the late endosomes and/or lysosomes and favors recycling from the endosomes to the plasma membrane. Thus, Tα1 facilitates proper folding and trafficking of p.Phe508del-CFTR and also stabilizes the rescued CFTR mutant protein at the plasma membrane.

### Tα1 rescues CFTR protein through USP36 deubiquitination and autophagy

Next, we measured the half-life of p.Phe508del-CFTR in CFBE41o-cells treated with Tα1 for 24 h at 37 °C. Tα1 did not increase steady-state CFTR mRNA expression (data not shown) and marginally

affected the half-life of wild-type (WT) CFTR, but it significantly increased the half-life of p.Phe508del-CFTR, which was shorter (1 h) than that of WT CFTR (4 h) (Fig. 3a,b). The effect of Tα1 could not be traced to inhibition of the proteasomal and lysosomal degradation pathways, as Tα1 did not inhibit degradation of reporter substrates (Supplementary Fig. 4a,b). However, Tα1 was detected in immunoprecipitated p.Phe508del-CFTR from CFBE41o- cells that overexpressed Tα1 or were treated with Tα1 for 2 h at 37 °C. While present in bronchial epithelial cells expressing WT CFTR, Tα1 was not detected in immunoprecipitated WT CFTR (Supplementary Fig. 5a,b). Overexpression of Tα1 increased CFTR maturation

(Supplementary Fig. 5c) and *IL10* expression and decreased *IL6* expression (Supplementary Fig. 5d), suggesting functional  $T\alpha 1$  activity. In accordance with the ER localization of  $T\alpha 1$  that is different from

that of its precursor, prothymosin<sup>37</sup>, these results indicate that  $T\alpha 1$  associates with p.Phe508del-CFTR, suggesting a chaperone activity of  $T\alpha 1$  that may affect the protein's ER quality control and degradation.

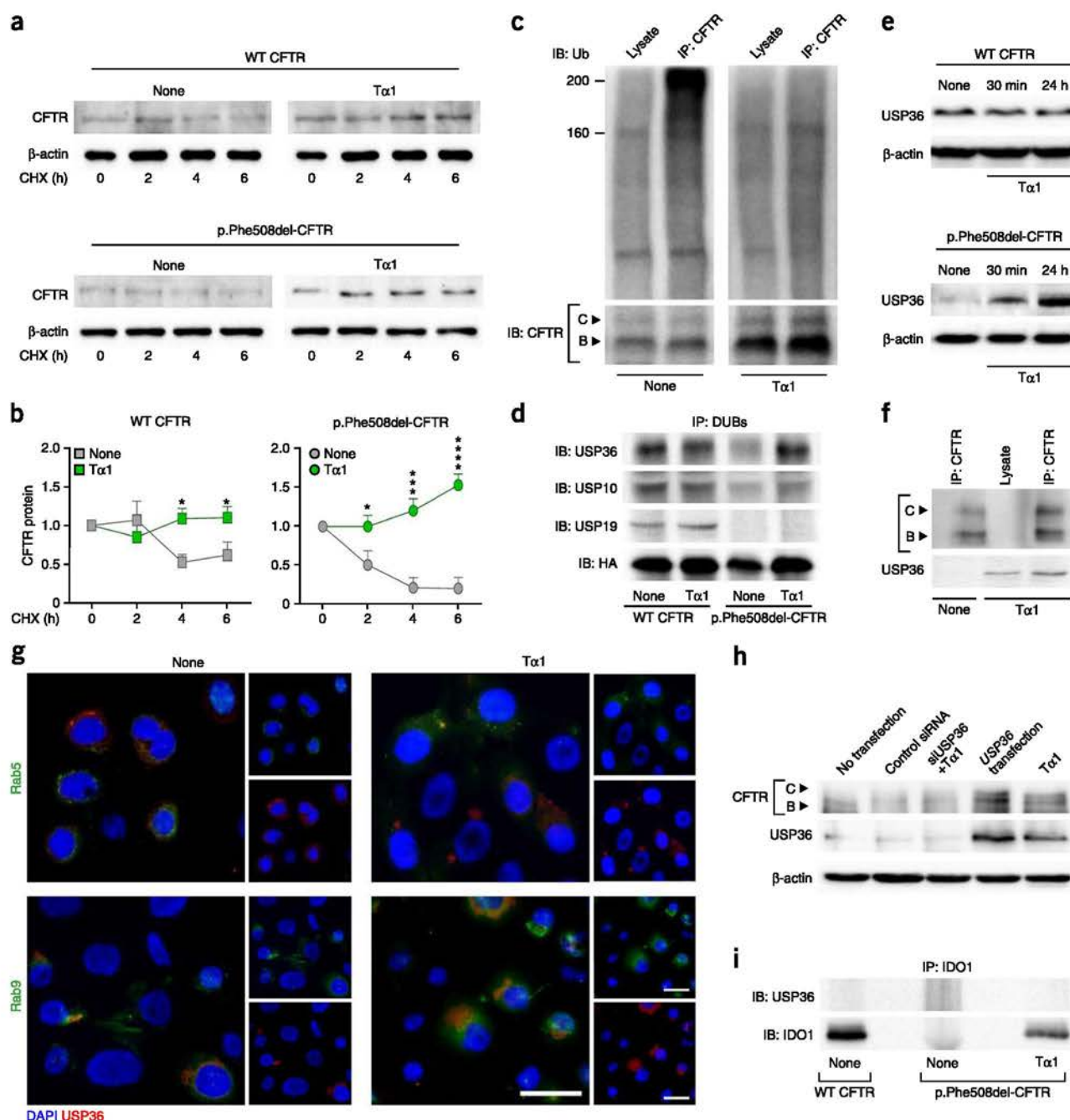


**Figure 3**  $T\alpha 1$  rescues p.Phe508del-CFTR by promoting USP36 deubiquitination. (a, b) Representative immunoblots ( $n = 3$ ) (a) and corresponding densitometric analysis (b) of CFTR in lysates from CFBE41o- cells transfected with WT CFTR or p.Phe508del-CFTR and treated with 100 ng/ml  $T\alpha 1$  for 24 h at 37 °C and cycloheximide (CHX) for up to 6 h. (c) Representative immunoblots (IB) of ubiquitin (Ub) in total lysates and lysates in which CFTR was immunoprecipitated (IP) from CFBE41o- cells treated with  $T\alpha 1$  for 2 h ( $n = 3$ ). (d) Representative immunoblots of HA and USP proteins in lysates from CFBE41o- cells expressing HA-Ub-VME in which the HA probe was immunoprecipitated ( $n = 3$ ). (e, f) Representative immunoblots of USP36 in total lysates (e) or lysates in which CFTR was immunoprecipitated (f) from CFBE41o- cells transfected with WT CFTR or p.Phe508del-CFTR and treated with  $T\alpha 1$  for 30 min or 24 h ( $n = 3$ ). (g) Colocalization of USP36 with either Rab5 or Rab9 ( $n = 5$  images per treatment) in CFBE41o- cells treated with  $T\alpha 1$  for 2 h. Scale bars, 100  $\mu$ m. See Supplementary Figure 10 for colocalization coefficients. (h) Representative immunoblots of CFTR and USP36 ( $n = 3$ ) in CFBE41o- cells treated with siRNA specific to *USP36* or control siRNA (scrambled version of the siRNA target sequence) or transfected with plasmid encoding *USP36*. (i) Representative immunoblots of USP36 ( $n = 3$ ) in lysates in which IDO1 was immunoprecipitated from CFBE41o- cells transfected with WT CFTR or p.Phe508del-CFTR and treated with  $T\alpha 1$  at 37 °C for 2 h. Data are presented as means  $\pm$  s.d. \* $P < 0.05$ , \*\*\* $P < 0.001$ , \*\*\*\* $P < 0.0001$ , two-way ANOVA with Bonferroni post test.

T $\alpha$ 1 perturbed the physical interaction of p.Phe508del-CFTR with the ER chaperon Hsp70 but not with Hsp90 or calnexin, which are known to assist protein folding or degradation<sup>38</sup> (Supplementary Fig. 5e,f).

Poorly folded plasma membrane-bound CFTR is subjected to proteolysis by the ER-associated degradation mechanism via the cytosolic ubiquitin (Ub)-26S proteasome system. Ubiquitination was reduced in immunoprecipitated p.Phe508del-CFTR from CFBE41o- cells treated with T $\alpha$ 1 (Fig. 3c). Most of the ubiquitinated p.Phe508del-CFTR was ~200 kDa in molecular weight. Because the CFTR detected by western blotting was in an ~180 kDa complex and a single ubiquitin has a molecular mass of 8 kDa, it appears that T $\alpha$ 1 reduced multiubiquitination, a signal that targets proteins in early endosomes for lysosomal degradation.

The removal of ubiquitin by deubiquitinating enzymes (DUBs) regulates sorting of ubiquitinated plasma membrane-associated proteins<sup>39</sup>. Using a hemagglutinin-tagged ubiquitin probe engineered to form an irreversible covalent bond with active DUBs<sup>35</sup>, we identified ubiquitin-specific protease 36 (USP36)—which inhibits autophagy of protein aggregates by deubiquitination<sup>40</sup>—as a regulator of deubiquitination events triggered by T $\alpha$ 1. Neither USP36—nor either of the two major p.Phe508del-CFTR DUBs, USP10 (ref. 35) and USP19 (ref. 41)—could be detected in T $\alpha$ 1-treated cells (Fig. 3d). Paralleling the promotion of mature CFTR (Fig. 2), the induction of USP36 occurred at 30 min after initial exposure and was still present at 24 h of exposure (Fig. 3e). USP36 associated with immunoprecipitated p.Phe508del-CFTR (Fig. 3f) and deubiquitinated CFTR in Rab5<sup>+</sup> endosomes and even more so in Rab9<sup>+</sup> endosomes in T $\alpha$ 1-treated cells (Fig. 3g). This is in line with the finding that Rab9 enters the endosomal pathway at the transition stage between early Rab5<sup>+</sup> and late Rab7<sup>+</sup> endosomes and colocalizes to the *trans*-Golgi network<sup>42</sup>. Depletion of USP36 by RNA interference abrogated the rescuing effect of T $\alpha$ 1 on mature p.Phe508del-CFTR, whereas its overexpression further increased the capacity of T $\alpha$ 1 to rescue mutated CFTR (Fig. 3h). Thus, the corrector activity of T $\alpha$ 1 correlated with USP36-mediated deubiquitination of CFTR in endosomes, thereby promoting CFTR trafficking to the post-endocytic compartment and more efficient ER export to the cell surface. USP36 was not involved in promotion of IDO1 activity by T $\alpha$ 1 (Fig. 3i), a finding consistent with the importance of the proteasomal degradation pathway for IDO1 activity<sup>21</sup> and, likewise, arguing for USP36 selectivity in CFTR correction.

The ubiquitin system is deeply influenced by autophagy<sup>43</sup>. Defective autophagy in CF leads to an increased pool of ubiquitinated proteins, including the ubiquitin-binding protein SQSTM1/p62, which is pivotal in the aggresome sequestration of ubiquitinated p.Phe508del-CFTR as well as in p.Phe508del-CFTR disposal from the plasma membrane after rescue<sup>32</sup>. Enforced expression of SQSTM1/p62 lacking the UBA domain stabilizes p.Phe508del-CFTR at the plasma membrane and promotes its recycling<sup>10</sup>. In accordance with the ability of autophagy to rescue CFTR function<sup>9</sup>, T $\alpha$ 1 was able to promote IDO1-dependent autophagy (Supplementary Fig. 6a–d), to reduce SQSTM1/p62 levels (Supplementary Fig. 6e) and, notably, to correct CFTR in an autophagy-dependent manner, as indicated by the decreased rescue activity in mice bearing *Cftr*<sup>F508del</sup> in a *Becn1*<sup>+/-</sup> haploinsufficient background, which confers a major autophagy defect<sup>9</sup> (Supplementary Fig. 6f).

### T $\alpha$ 1 increases p.Phe508del-CFTR and CLCA1 function

The corrector and stabilizing capacity of T $\alpha$ 1 would anticipate increased chloride ion channel function of the rescued p.Phe508del-CFTR.

We treated p.Phe508del-CFTR-transfected CFBE41o- cells with T $\alpha$ 1 for either 2 or 24 h at 37 °C before determining the channel open probability ( $P_o$ ) of p.Phe508del-CFTR. Studies have estimated that the extent of correction in p.Phe508del airway epithelial cells must approximate 20–30% of WT CFTR function to provide therapeutic benefit<sup>44</sup>. Treatment with T $\alpha$ 1 for 2 h restored channel gating of rescued p.Phe508del-CFTR (Fig. 4a) with a fourfold increase in  $P_o$ , namely, from  $0.08 \pm 0.02$  of untreated CFTR to  $0.35 \pm 0.07$  after treatment (Fig. 4b), with the latter  $P_o$  values being similar to those for WT CFTR<sup>45</sup>. A twofold increase in chloride current density was still observed at 24 h after treatment as assessed by whole-cell patch-clamp recordings of cells expressing p.Phe508del-CFTR (Fig. 4c,d), and the rate of iodide efflux would then approximate 70% of the control value in WT cells, as assessed by the halide-sensitive fluorescent probe 6-methoxy-*N*-(sulfo-propyl)quinolinium after stimulation with forskolin (Fig. 4e). This was confirmed by the results obtained in human bronchial epithelial (HBE) cells from a subject with two distinct mutations, p.Gly1244Glu and p.Phe508del, whereby a gating defect<sup>46</sup> occurred in association with the p.Phe508del defect. The effect of T $\alpha$ 1 was qualitatively similar, although of a lesser extent, to that obtained with potentiator ivacaftor (Fig. 4f), which is known to restore channel activity in CFTR gating (class III) mutations, including the p.Gly1244Glu mutation<sup>47</sup>. This is in agreement with recent evidence indicating that proteostasis regulators rescue functional CFTR expression in human and mouse cells bearing only one copy of the p.Phe508del allele<sup>9</sup>.

Bypassing CFTR by targeting additional ion channels is an alternative strategy to circumvent the CFTR defect<sup>48</sup>. On the basis of data gathered from *in vivo* DNA microarray analysis of T $\alpha$ 1-treated mice (Supplementary Fig. 7a,b), we assessed whether T $\alpha$ 1 would increase mRNA expression of the calcium-activated chloride channel regulator 1 (CLCA1), a member of the CLCA protein family capable of paracrine modulation of the activity of TMEM16A<sup>49</sup>, an alternative chloride channel that could obviate the primary defect in CF<sup>48</sup>. T $\alpha$ 1 potentiated calcium-activated chloride currents (Fig. 4g,h) and persistently increased the expression of CLCA1 (Fig. 4i) in CFBE41o- cells. Depleting CLCA1 with specific small interfering RNAs (siRNAs) (Supplementary Fig. 7) greatly reduced the ion channel activity promoted by T $\alpha$ 1 (Fig. 4e). These findings suggested that T $\alpha$ 1 is endowed with effects that can further ameliorate chloride channel activity in CF.

### T $\alpha$ 1 rescues p.Phe508del-CFTR in mice and HBE cells

To determine whether T $\alpha$ 1 corrects CFTR *in vivo*, we assessed CFTR expression and activity in *Cftr*<sup>F508del</sup> C57BL/6 mice aged 4 weeks treated daily for 6 d with 200  $\mu$ g of T $\alpha$ 1 per kg of bodyweight. T $\alpha$ 1 restored CFTR expression in the lung (Fig. 5a,b) and small intestine (Fig. 5c,d), as assessed by immunoblotting of cell lysates (Fig. 5a,c), and it promoted localization of mature CFTR to the plasma membrane (Fig. 5b,d), as revealed by immunohistochemistry. Functionally, T $\alpha$ 1 treatment restored channel gating in lung epithelial cells with a twofold increase in  $P_o$  from  $0.23 \pm 0.02$  before stimulation to  $0.45 \pm 0.04$  after forskolin and genistein stimulation (Fig. 5e,f). In intestines from *Cftr*<sup>F508del</sup> mice mounted in Ussing chambers, T $\alpha$ 1 significantly increased CFTR-dependent chloride ion conductance in response to forskolin, much like the proteostasis regulator cysteamine<sup>9</sup> (Fig. 5g). Rescue of CFTR activity by T $\alpha$ 1 was also observed in *Cftr*<sup>F508del</sup> mice on an FVB/129 background (data not shown). Of interest, T $\alpha$ 1 also increased CLCA1 expression in both the lung (Fig. 5h,i) and the gut

**Q36** (Fig. 5j,k) of *Cftr*<sup>F508del</sup> mice. Taken together, these data indicated that administration of Tα1 ameliorated chloride ion fluxes in the intestinal and respiratory tracts of *Cftr*<sup>F508del</sup> mice.

To test the activity of Tα1 in a more relevant clinical setting, HBE cells from five subjects homozygous for the p.Phe508del-CFTR mutation were assessed for CFTR, USP36 protein levels and *CLCA1* gene

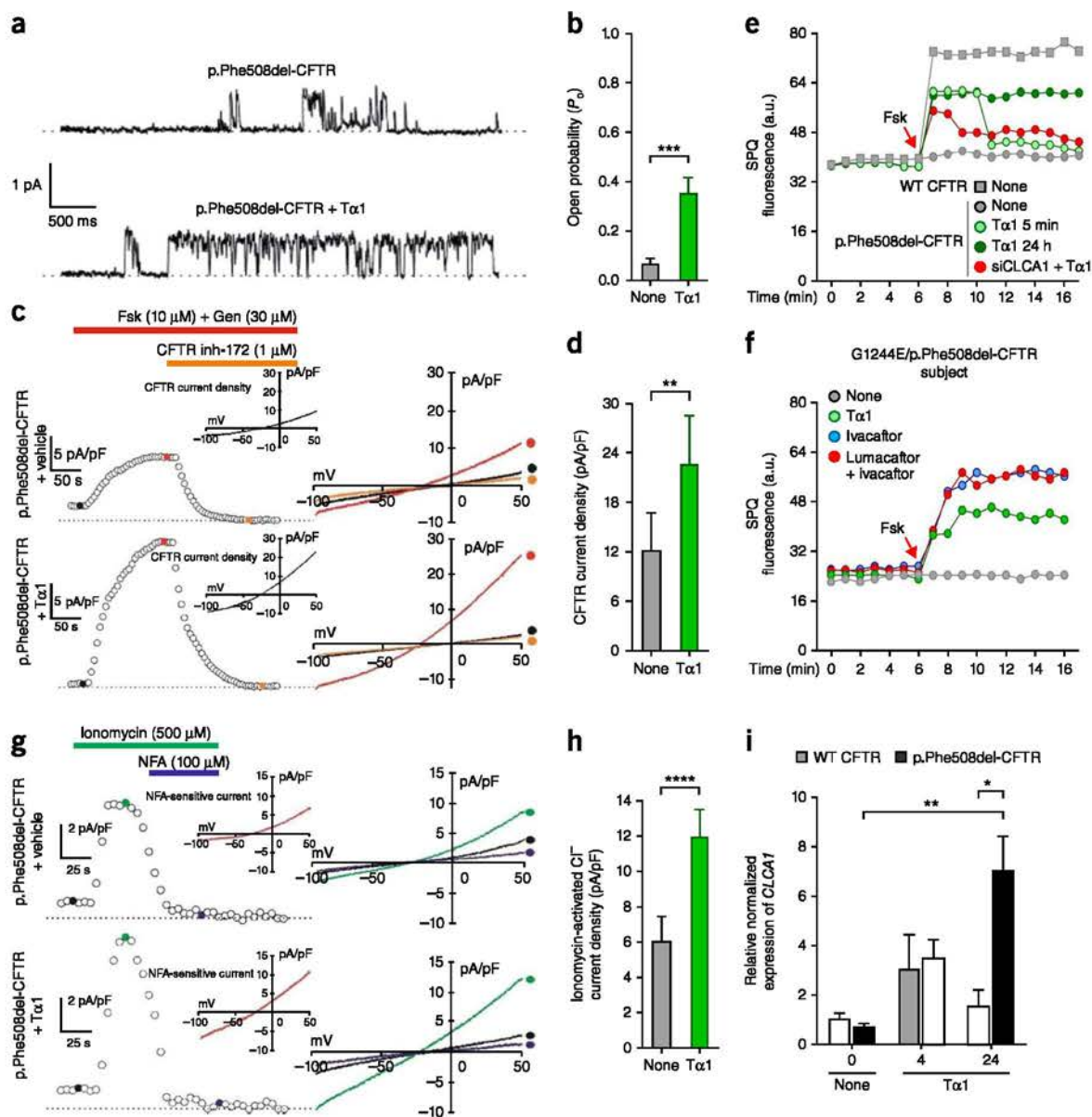


**Figure 4** Tα1 rescues p.Phe508del-CFTR functional activity. (a) CFTR single-channel currents recorded at +100 mV from p.Phe508del-CFTR-transfected CFBE41o- cells treated with 100 ng/ml Tα1 or vehicle for 2 h (dotted lines correspond to the channel's closed state). (b)  $P_o$  calculated at +100 mV ( $n = 4$ ;  $***P < 0.001$ , Student's  $t$ -test). (c) Time course of whole-cell CFTR current densities induced by forskolin (Fsk) + genistein (Gen) at +50 mV in p.Phe508del-CFTR-transfected CFBE41o- cells treated with 100 ng/ml Tα1 or vehicle for 24 h followed by blockade with CFTR inhibitor 172 (CFTR inh-172). The horizontal bars indicate the time period of drug application (left). Current-voltage ( $I$ - $V$ ) relationships were elicited by ramps from -100 mV to +50 mV (holding potential, -40 mV) and are constructed for the time points corresponding to the colored dots (right). CFTR inhibitor 172-sensitive chloride current densities were calculated by subtracting the residual current density recorded after the application of CFTR inhibitor 172 from the current density induced by forskolin and genistein (insets). (d) Average CFTR current density induced by forskolin and genistein ( $n = 8$ ;  $**P < 0.01$ , Student's  $t$ -test). (e) Iodide efflux assessed by a fluorescence assay (SPQ) upon forskolin stimulation of CFBE41o- cells transfected with WT CFTR or p.Phe508del-CFTR and treated with Tα1 at 37 °C ( $n = 3$ ). Treatment with siRNA targeting *CLCA1* or control siRNA was performed 24 h before Tα1 addition for 5 min only. (f) Iodide efflux in cells treated with Tα1 or with ivacaftor alone or in combination with lumacaftor for 24 h at 37 °C ( $n = 3$ ). (g) Time course of ionomycin-induced calcium-activated chloride current densities at +50 mV in CFBE41o- cells transfected with WT CFTR or p.Phe508del-CFTR and treated with Tα1 at 37 °C ( $n = 5$ ). (h) Average current density ( $n = 8$ ;  $****P < 0.0001$ , Student's  $t$ -test). (i) *CLCA1* expression as determined by RT-PCR in CFBE41o- cells transfected with WT CFTR or p.Phe508del-CFTR and treated with Tα1 at 37 °C ( $n = 5$ ).  $*P < 0.05$ ,  $**P < 0.01$ , two-way ANOVA with Bonferroni post test. Data are presented as means  $\pm$  s.d. For statistical analysis, see **Supplementary Figure 10**.

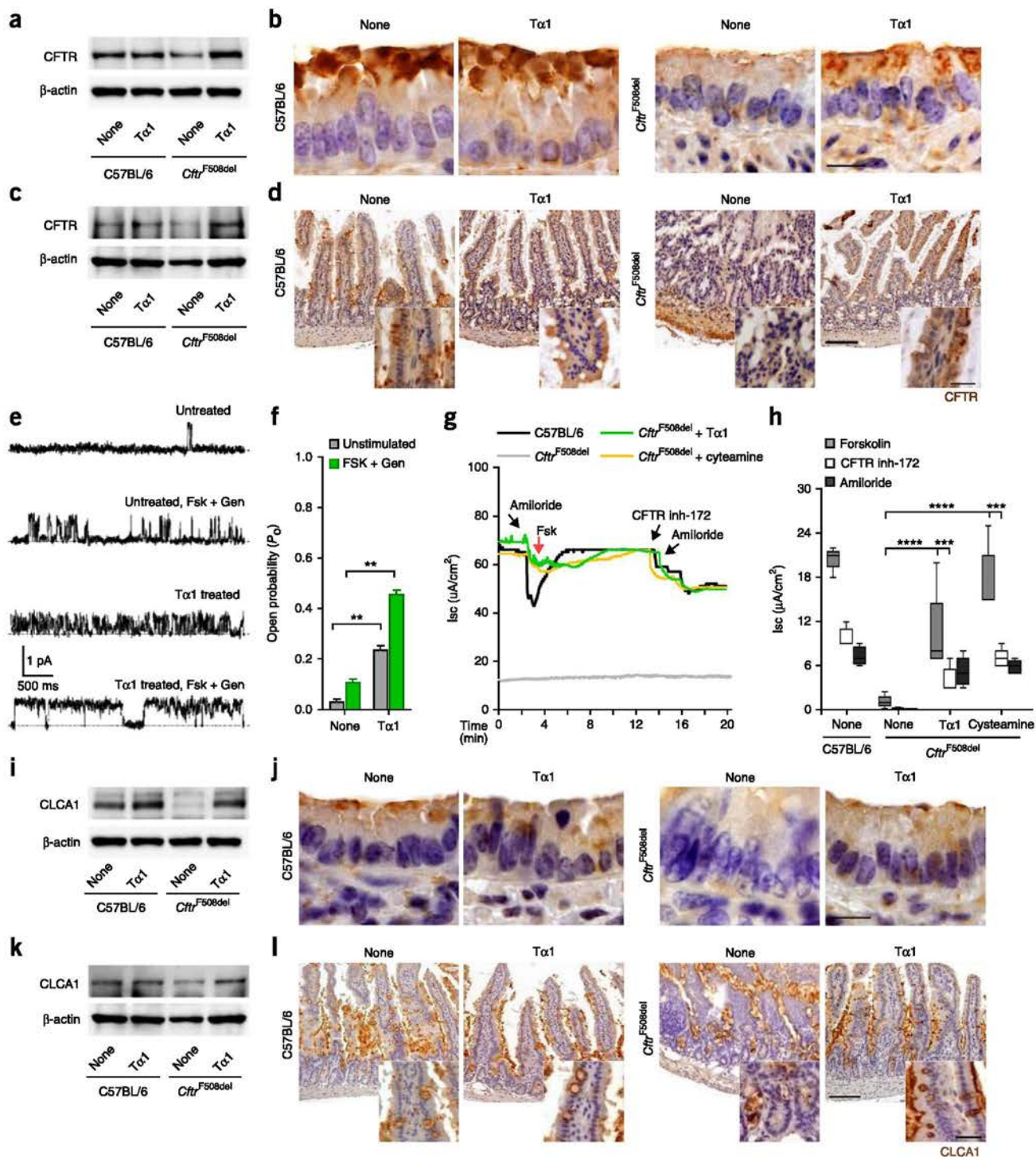


**Figure 5** T $\alpha$ 1 rescues p.Phe508del-CFTR activity in *Cfr*<sup>F508del</sup> mice. (a–d) Control C57BL/6 and *Cfr*<sup>F508del</sup> mice were treated with 200  $\mu$ g per kg bodyweight T $\alpha$ 1 intraperitoneally for 6 d before the assessment of CFTR protein expression in the lung (a,b) and small intestine (c,d) by immunoblotting of lysates ( $n = 3$ ) (a,c) and immunohistochemistry ( $n = 5$  images per mouse) (b,d). Scale bars, 25  $\mu$ m in b, 200  $\mu$ m in d, and 100  $\mu$ m in the inset. (e) CFTR single-channel currents recorded at +100 mV from ex vivo purified epithelial cells in response to forskolin and genistein ( $n = 4$ ) (dotted lines represent the zero-current baseline when the channel is in its closed state). (f)  $P_o$  of channels calculated at +100 mV ( $n = 4$ ). (g,h) Ex vivo ileum-mounted cells from C57BL/6 and *Cfr*<sup>F508del</sup> mice were placed in Ussing chambers in the presence of CFTR inhibition (CFTR inhibitor 172) and amiloride. Cysteamine was used as a positive control. (g) CFTR-dependent chloride secretion measured by means of the forskolin-induced increase in the chloride current (Isc). (h) Summary of the results in g ( $n = 4$ ). (i–l) Control C57BL/6 and *Cfr*<sup>F508del</sup> mice were treated with 200  $\mu$ g per kg bodyweight T $\alpha$ 1 intraperitoneally, and CLCA1 protein expression in lung (i,j) and small intestine (k,l) was assessed by immunoblotting of lysates (i,k) and immunohistochemistry ( $n = 5$  images per mouse) (j,l). Scale bars, 25  $\mu$ m in j, 200  $\mu$ m in l, and 100  $\mu$ m in the insets. Immunoblotting and immunohistochemical sections are representative of three independent experiments with  $n = 6$  mice per group. Data are presented as means  $\pm$  s.d. \*\* $P < 0.01$ , \*\*\* $P < 0.001$ , \*\*\*\* $P < 0.0001$ , two-way ANOVA with Bonferroni post test.

Q103  
Q104  
Q106  
Q108

Q105  
Q107

Q109  
Q110



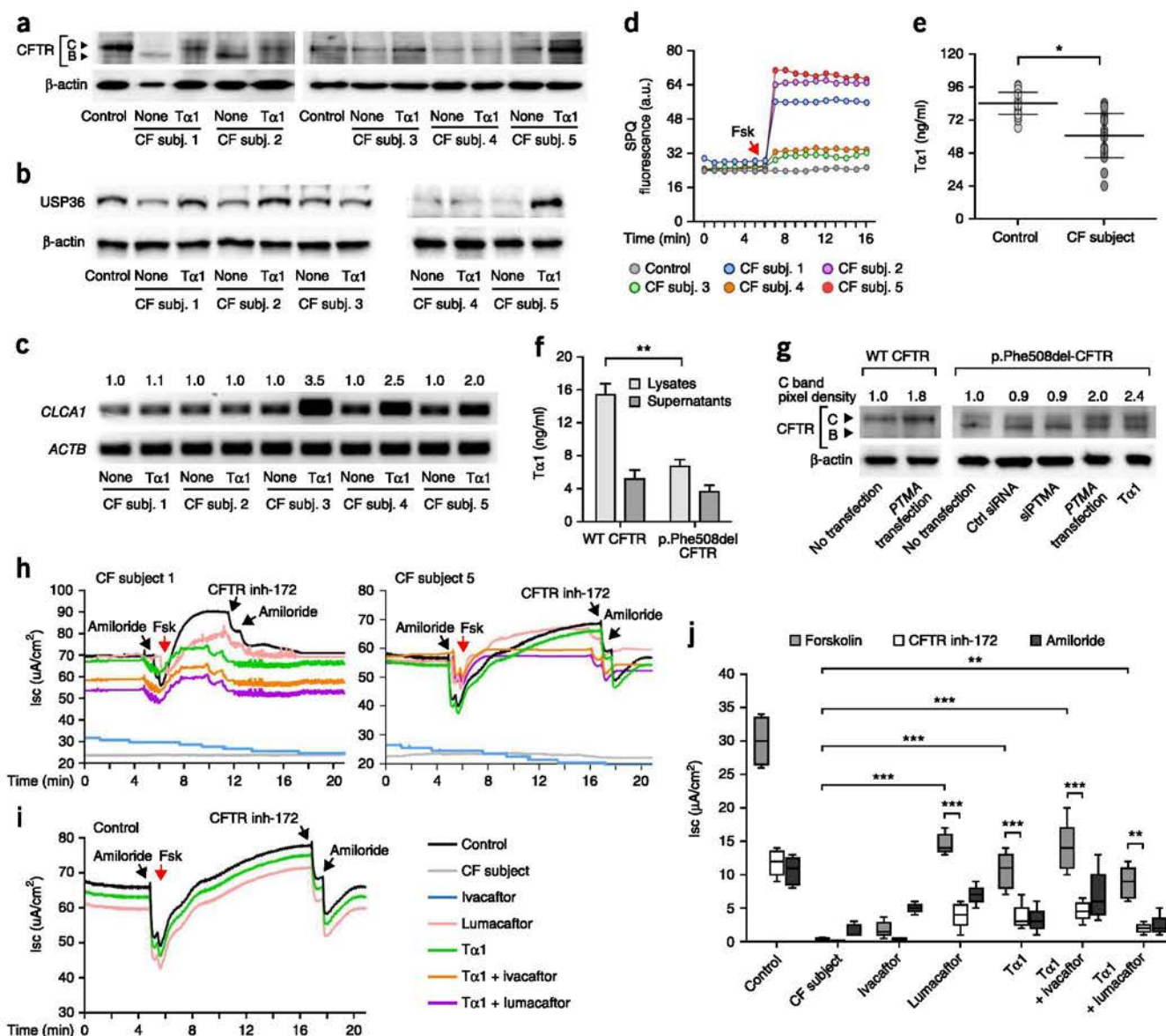


**Figure 6** T $\alpha$ 1 rescues p.Phe508del-CFTR activity in CF cells and human bronchial epithelial cells from subjects with CF. (a–d) Representative CFTR (a) and USP36 (b) protein expression ( $n = 3$ ) and *CLCA1* gene expression ( $n = 3$ ) (c), and iodide efflux as assessed by SPQ assay upon stimulation with forskolin (d) in HBE cells from five subjects (subj.) with the p.Phe508del mutation and controls treated with 100 ng/ml T $\alpha$ 1 for 24 h at 37 °C. (e,f) T $\alpha$ 1 production in sputa from controls and subjects with CF ( $n = 3$ ; \* $P < 0.05$ , Student's *t*-test) (e) and lysates or supernatants from CFBE41o-cells transfected with WT CFTR or p.Phe508del-CFTR ( $n = 3$ ; \*\* $P < 0.01$ , two-way ANOVA with Bonferroni post test). (g) Representative immunoblots ( $n = 3$ ) of CFTR and C band pixel density in cells transfected with siRNA targeting *PTMA* (prothymosin) or plasmid encoding *PTMA* and treated with T $\alpha$ 1 at 37 °C for 2 h. (h–j) CFTR-dependent chloride secretion measured by means of forskolin-induced increase in the Isc in HBE cells from two subjects with CF (h) and controls (i) treated with T $\alpha$ 1, ivacaftor or lumacaftor for 24 h at 37 °C and mounted in Ussing chambers in the presence of CFTR inhibition (CFTR inh-172) and amiloride. (j) Summary of the results in h and i ( $n = 4$ ). Data are presented as means  $\pm$  s.d. \*\* $P < 0.01$ , \*\*\* $P < 0.001$ , two-way ANOVA with Bonferroni post test.

expression after exposure to T $\alpha$ 1 for 24 h at 37 °C. T $\alpha$ 1 increased expression of the mature p.Phe508del-CFTR protein (Fig. 6a), USP36 (Fig. 6b) and *CLCA1* (Fig. 6c) in three of the five subjects with CF and concomitantly increased ion channel activity (Fig. 6d). To assess the clinical relevance of these findings, we measured the concentrations of T $\alpha$ 1 in sputa from subjects with the p.Phe508del-CFTR mutation and control subjects, taking into consideration that T $\alpha$ 1 is highly expressed not only in human thymic epithelium<sup>50</sup> but also in peripheral tissues<sup>33</sup>. We found lower concentrations of T $\alpha$ 1 in subjects with CF than in controls (Fig. 6e), which is consistent with the lower levels observed

in supernatants and lysates from p.Phe508del-CFTR-transfected CFBE41o-cells relative to cells transfected with WT CFTR (Fig. 6f). Because signaling via TLRs influences T $\alpha$ 1 production by lung epithelial cells (Supplementary Fig. 8), the deregulated TLR activity observed in subjects with CF<sup>13</sup> may affect local T $\alpha$ 1 production and, ultimately, CFTR activity. This likely occurs, as endogenous T $\alpha$ 1 affected functional expression of CFTR. We assessed the expression of mature CFTR in HBE cells from subjects with the p.Phe508del-CFTR mutation and controls after prothymosin depletion (by specific siRNA) or overexpression (via transfection) because T $\alpha$ 1 is produced

by cleavage of prothymosin by the lysosomal asparaginyl endopeptidase legumain<sup>37</sup>. We found that mature p.Phe508del-CFTR expression was negated by prothymosin inhibition and increased by prothymosin overexpression (Fig. 6g). Of interest, prothymosin overexpression also increased mature CFTR expression in cells from controls (Fig. 6g), which points to a role for the endogenous prothymosin/T $\alpha$ 1 system in CFTR physiology.

We finally comparatively assessed the ion channel activity of T $\alpha$ 1 with that of lumacaftor or ivacaftor, either alone or in combination, in primary HBE cells from controls or subjects homozygous for the p.Phe508del-CFTR mutation. Ussing chamber tracings revealed that T $\alpha$ 1 promoted the forskolin-induced increase in the chloride current (I<sub>sc</sub>) in HBE cells from subjects with CF (Fig. 6h) but not controls (Fig. 6i), an effect that was sensitive to CFTR inhibition and was similar to that observed with lumacaftor. With the only exception of subject 8 (Supplementary Fig. 9), the activity of T $\alpha$ 1 was not additive to that of ivacaftor, which is unable to rescue p.Phe508del-CFTR at the plasma membrane<sup>47</sup>. Similar results were obtained by means of a halide-sensitive fluorescent probe (Supplementary Fig. 9). In spite of the reported interindividual variability, even in patients bearing the same genotype, these results suggest that T $\alpha$ 1 alone or in combination can be used for treating subjects with the p.Phe508del-CFTR mutation.

## DISCUSSION

While regulation of lung homeostasis and inflammation by CFTR is an established notion<sup>51</sup>, whether regulation of inflammation will affect CFTR functioning is less clear. Here we show that T $\alpha$ 1 is endowed with the unique ability to correct CFTR defects through the regulation of inflammation. Although T $\alpha$ 1 appears to have a multitasking chaperon activity through which it may affect the balance of protein folding versus degradation (for example, by associating with p.Phe508del-CFTR, perturbing the interaction of mutated CFTR with the ER chaperons and activating USP36-mediated deubiquitination of misfolded CFTR), the induction of IDO1 appears to be key to this mechanism. IDO1 is known to play a major role in preventing excessive pathology in immune-mediated tissue injury through multiple effector mechanisms, including the induction of autophagy<sup>31</sup>. In accordance with the ability of autophagy to rescue CFTR function<sup>9</sup>, the promotion of autophagy appeared to contribute to the corrector activity of T $\alpha$ 1 and qualified T $\alpha$ 1 as a proteostasis regulator that rectifies an unbalanced degradasome activity in CF cells. Proteostasis regulators, such as cysteamine, have emerged as a new option for CFTR repair by avoiding unwanted protein–protein interactions, favoring the trafficking and stability of mutant CFTR and hence controlling inflammation<sup>9,10,32</sup>. Unlike cysteamine, the anti-inflammatory effects of T $\alpha$ 1 are not dependent on an ability to rescue functional p.Phe508del-CFTR, as they also occur in CFTR-knockout mice. Therefore, T $\alpha$ 1 is an excellent example of a drug with primary anti-inflammatory effects that can also favor rescue of p.Phe508del-CFTR.

The cross-regulation between autophagy and inflammasomes<sup>52</sup> may also explain the ability of T $\alpha$ 1 to inhibit NLRP3-based inflammasome activity, which is known to contribute to respiratory infections and pathologic airway inflammation in CF<sup>28</sup>. Moreover, as immune tolerance induced by IDO1 encompasses an activity on tissue repair and remodeling<sup>53</sup>, this may explain the remarkable effect of T $\alpha$ 1 in restoring host tissue architecture in the lung and the gastrointestinal tract of *Cftr*<sup>F508del</sup> mice. Similarly to subjects with CF<sup>30</sup>, an altered pulmonary histopathophysiology is present in those mice in the absence

of infection<sup>54</sup>. Altogether, these findings may point to T $\alpha$ 1 as a drug candidate capable of preventing CF progression at very early stages of the disease.

Through its multitasking activity, T $\alpha$ 1 may represent a proper means of rectifying the multifunctional defect in individuals with CF, including the increase in CLCA1 activity. Both clinical and animal model studies have suggested a compensatory role for CLCA1 in CF<sup>55,56</sup>. Even though calcium-activated chloride channels are abundant in mouse but not in human airways<sup>48,57</sup>, mutations in CLCA1 are found in a subset of people with CF marked by aggravated intestinal disease<sup>55</sup>, a finding consistent with the observation that calcium-activated chloride channels are defective in the intestine of individuals with CF<sup>57</sup>. This may explain the remarkable activity of T $\alpha$ 1 in the gastrointestinal tract of *Cftr*<sup>F508del</sup> mice, in which chloride channel activity was rectified. This indicates that T $\alpha$ 1 could be clinically exploited for pharmacologic correction of defective CFTR not only in the lung but also in the gut, implying that gastrointestinal outcome measures could be promising clinical endpoints of T $\alpha$ 1 therapeutics.

Only a combination of molecules with different mechanisms of action is expected to induce a significant degree of p.Phe508del-CFTR correction, as shown by the combination of ivacaftor with lumacaftor<sup>6,58</sup> or VX-661 (refs. 59,60). Although the corrector activity of T $\alpha$ 1 has yet to be verified relative to the agents moving into development in the clinic, the excellent safety profile and cost effectiveness of Zadaxin in adults and children<sup>20</sup> suggest that T $\alpha$ 1 could be tested in clinical trials for possible pulmonary and extrapulmonary benefits in individuals with CF.

**URLs.** List of CF-associated mutations, <http://www.genet.sickkids.on.ca/cftr/StatisticsPage.html>.

## METHODS

Methods, including statements of data availability and any associated accession codes and references, are available in the online version of the paper.

*Note: Any Supplementary Information and Source Data files are available in the online version of the paper.*

## ACKNOWLEDGMENTS

We thank the primary cell culture service offered from the Italian Cystic Fibrosis Research Foundation for kindly providing us with the HBE cells. We thank B. Scholte (Erasmus Medical Center Rotterdam), who provided *Cftr*<sup>tm1EUR</sup> mice (F508del mice, European Economic Community European Coordination Action for Research in Cystic Fibrosis program EU FP6 SHMCT-2005-018932). This study was supported by the Specific Targeted Research Project FunMeta (ERC-2011-AdG-293714 to L.R.). M.P. gratefully acknowledges a fellowship from the Italian Cystic Fibrosis Research Foundation.

## AUTHOR CONTRIBUTIONS

V.O., R.G.I. and M.P. performed most immunoblotting and immunofluorescence experiments; R.G.I., M.B., S.M. and E.F. performed murine *in vivo* experiments; M.C.D'A., L.S. and M.P. performed electrophysiology experiments; E.F. and M.T.P. performed TLR9 colocalization experiments; M.M.B. and G.S. performed transfection experiments; V.R.V. performed Ussing chamber experiments; and A.L.G., L.M., G.K., M.P., P.P., E.G. and L.R. designed the experiments, analyzed the data and wrote the paper.

## COMPETING FINANCIAL INTERESTS

The authors declare competing financial interests; details are available in the online version of the paper.

Reprints and permissions information is available online at <http://www.nature.com/reprints/index.html>.

1. Rowe, S.M., Miller, S. & Sorscher, E.J. Cystic fibrosis. *N. Engl. J. Med.* **352**, 1992–2001 (2005).

2. Lukacs, G.L. & Verkman, A.S. CFTR: folding, misfolding and correcting the  $\Delta F508$  conformational defect. *Trends Mol. Med.* **18**, 81–91 (2012).
3. Okiyoneda, T. *et al.* Peripheral protein quality control removes unfolded CFTR from the plasma membrane. *Science* **329**, 805–810 (2010).
4. Pedemonte, N. *et al.* Small-molecule correctors of defective  $\Delta F508$ -CFTR cellular processing identified by high-throughput screening. *J. Clin. Invest.* **115**, 2564–2571 (2005).
5. Galletta, L.J. Managing the underlying cause of cystic fibrosis: a future role for potentiators and correctors. *Paediatr. Drugs* **15**, 393–402 (2013).
6. Wainwright, C.E., Elborn, J.S. & Ramsey, B.W. Lumacaftor-ivacaftor in patients with cystic fibrosis homozygous for Phe508del CFTR. *N. Engl. J. Med.* **373**, 1783–1784 (2015).
7. Quon, B.S. & Rowe, S.M. New and emerging targeted therapies for cystic fibrosis. *Br. Med. J.* **352**, i859 (2016).
8. Hegde, R.N. *et al.* Unravelling druggable signalling networks that control F508del-CFTR proteostasis. *eLife* **4**, e10365 (2015).
9. Tosco, A. *et al.* A novel treatment of cystic fibrosis acting on-target: cysteamine plus epigallocatechin gallate for the autophagy-dependent rescue of class II-mutated CFTR. *Cell Death Differ.* **23**, 1380–1393 (2016).
10. Villella, V.R. *et al.* Disease-relevant proteostasis regulation of cystic fibrosis transmembrane conductance regulator. *Cell Death Differ.* **20**, 1101–1115 (2013).
11. Cantin, A.M., Hartl, D., Konstan, M.W. & Chmiel, J.F. Inflammation in cystic fibrosis lung disease: pathogenesis and therapy. *J. Cyst. Fibros.* **14**, 419–430 (2015).
12. Rubin, B.K. Cystic fibrosis: myths, mistakes, and dogma. *Paediatr. Respir. Rev.* **15**, 113–116 (2014).
13. Cohen, T.S. & Prince, A. Cystic fibrosis: a mucosal immunodeficiency syndrome. *Nat. Med.* **18**, 509–519 (2012).
14. Hoffman, L.R. & Ramsey, B.W. Cystic fibrosis therapeutics: the road ahead. *Chest* **143**, 207–213 (2013).
15. de Benedictis, F.M. & Bush, A. Corticosteroids in respiratory diseases in children. *Am. J. Respir. Crit. Care Med.* **185**, 12–23 (2012).
16. Devor, D.C. & Schultz, B.D. Ibuprofen inhibits cystic fibrosis transmembrane conductance regulator-mediated Cl<sup>-</sup> secretion. *J. Clin. Invest.* **102**, 679–687 (1998).
17. Goldstein, A.L. & Goldstein, A.L. From lab to bedside: emerging clinical applications of thymosin  $\alpha 1$ . *Expert Opin. Biol. Ther.* **9**, 593–608 (2009).
18. Romani, L. *et al.* Thymosin  $\alpha 1$  activates dendritic cell tryptophan catabolism and establishes a regulatory environment for balance of inflammation and tolerance. *Blood* **108**, 2265–2274 (2006).
19. Mandaliti, W. *et al.* New studies about the insertion mechanism of thymosin  $\alpha 1$  in negative regions of model membranes as starting point of the bioactivity. *Amino Acids* **48**, 1231–1239 (2016).
20. Tuthill, C.V. & King, R.S. Thymosin  $\alpha 1$ —a peptide immune modulator with a broad range of clinical applications. *Clin. Exp. Pharmacol.* **3**, 133 (2013).
21. Puccetti, P. & Grohmann, U. IDO and regulatory T cells: a role for reverse signalling and non-canonical NF- $\kappa$ B activation. *Nat. Rev. Immunol.* **7**, 817–823 (2007).
22. Iannitti, R.G. *et al.* Th17/Treg imbalance in murine cystic fibrosis is linked to indoleamine 2,3-dioxygenase deficiency but corrected by kynurenines. *Am. J. Respir. Crit. Care Med.* **187**, 609–620 (2013).
23. Latz, E. *et al.* TLR9 signals after translocating from the ER to CpG DNA in the lysosome. *Nat. Immunol.* **5**, 190–198 (2004).
24. Bruscia, E. *et al.* Isolation of CF cell lines corrected at  $\Delta F508$ -CFTR locus by SFHR-mediated targeting. *Gene Ther.* **9**, 683–685 (2002).
25. King, J., Brunel, S.F. & Warris, A. *Aspergillus* infections in cystic fibrosis. *J. Infect.* **72** (Suppl. 1), S50–S55 (2016).
26. King, R.S. & Tuthill, C. Evaluation of thymosin  $\alpha 1$  in nonclinical models of the immune-suppressing indications melanoma and sepsis. *Expert Opin. Biol. Ther.* **15** (Suppl. 1), S41–S49 (2015).
27. Ancell, C.D., Phipps, J. & Young, L. Thymosin  $\alpha 1$ . *Am. J. Health Syst. Pharm.* **58**, 879–885; quiz 886–878 (2001).
28. Iannitti, R.G. *et al.* IL-1 receptor antagonist ameliorates inflammasome-dependent inflammation in murine and human cystic fibrosis. *Nat. Commun.* **7**, 10791 (2016).
29. Snouwaert, J.N. *et al.* An animal model for cystic fibrosis made by gene targeting. *Science* **257**, 1083–1088 (1992).
30. Stoltz, D.A., Meyerholz, D.K. & Welsh, M.J. Origins of cystic fibrosis lung disease. *N. Engl. J. Med.* **372**, 351–362 (2015).
31. McGaha, T.L. IDO-GCN2 and autophagy in inflammation. *Oncotarget* **6**, 21771–21772 (2015).
32. Luciani, A. *et al.* Defective CFTR induces aggresome formation and lung inflammation in cystic fibrosis through ROS-mediated autophagy inhibition. *Nat. Cell Biol.* **12**, 863–875 (2010).
33. Pica, F. *et al.* Serum thymosin  $\alpha 1$  levels in patients with chronic inflammatory autoimmune diseases. *Clin. Exp. Immunol.* **186**, 39–45 (2016).
34. Denning, G.M. *et al.* Processing of mutant cystic fibrosis transmembrane conductance regulator is temperature-sensitive. *Nature* **358**, 761–764 (1992).
35. Bomberger, J.M., Barnaby, R.L. & Stanton, B.A. The deubiquitinating enzyme USP10 regulates the post-endocytic sorting of cystic fibrosis transmembrane conductance regulator in airway epithelial cells. *J. Biol. Chem.* **284**, 18778–18789 (2009).
36. Gentsch, M. *et al.* Endocytic trafficking routes of wild type and  $\Delta F508$  cystic fibrosis transmembrane conductance regulator. *Mol. Biol. Cell* **15**, 2684–2696 (2004).
37. Sarandeses, C.S., Covelo, G., Diaz-Jullien, C. & Freire, M. Prothymosin  $\alpha$  is processed to thymosin  $\alpha 1$  and thymosin  $\alpha 11$  by a lysosomal asparaginyl endopeptidase. *J. Biol. Chem.* **278**, 13286–13293 (2003).
38. Heard, A., Thompson, J., Carver, J., Bekey, M. & Wang, X.R. Targeting molecular chaperones for the treatment of cystic fibrosis: is it a viable approach? *Curr. Drug Targets* **16**, 958–964 (2015).
39. Millard, S.M. & Wood, S.A. Riding the DUBway: regulation of protein trafficking by deubiquitylating enzymes. *J. Cell Biol.* **173**, 463–468 (2006).
40. Taillebourg, E. *et al.* The deubiquitinating enzyme USP36 controls selective autophagy activation by ubiquitinated proteins. *Autophagy* **8**, 767–779 (2012).
41. Hassink, G.C. *et al.* The ER-resident ubiquitin-specific protease 19 participates in the UPR and rescues ERAD substrates. *EMBO Rep.* **10**, 755–761 (2009).
42. Kucera, A. *et al.* Spatiotemporal resolution of Rab9 and Cl-MPR dynamics in the endocytic pathway. *Traffic* **17**, 211–229 (2016).
43. Lamark, T. & Johansen, T. Autophagy: links with the proteasome. *Curr. Opin. Cell Biol.* **22**, 192–198 (2010).
44. Zhang, L. *et al.* CFTR delivery to 25% of surface epithelial cells restores normal rates of mucus transport to human cystic fibrosis airway epithelium. *PLoS Biol.* **7**, e1000155 (2009).
45. Van Goor, F. *et al.* Correction of the F508del-CFTR protein processing defect *in vitro* by the investigational drug VX-809. *Proc. Natl. Acad. Sci. USA* **108**, 18843–18848 (2011).
46. Yu, H. *et al.* Ivacaftor potentiation of multiple CFTR channels with gating mutations. *J. Cyst. Fibros.* **11**, 237–245 (2012).
47. Van Goor, F., Yu, H., Burton, B. & Hoffman, B.J. Effect of ivacaftor on CFTR forms with missense mutations associated with defects in protein processing or function. *J. Cyst. Fibros.* **13**, 29–36 (2014).
48. Caputo, A. *et al.* TMEM16A, a membrane protein associated with calcium-dependent chloride channel activity. *Science* **322**, 590–594 (2008).
49. Sala-Rabanal, M., Yurtsever, Z., Nichols, C.G. & Brett, T.J. Secreted CLCA1 modulates TMEM16A to activate Ca<sup>2+</sup>-dependent chloride currents in human cells. *eLife* **4** <http://dx.doi.org/10.7554/eLife.05875> (2015).
50. Dalakas, M.C., Engel, W.K., McClure, J.E., Goldstein, A.L. & Askanas, V. Immunocytochemical localization of thymosin- $\alpha 1$  in thymic epithelial cells of normal and myasthenia gravis patients and in thymic cultures. *J. Neurol. Sci.* **50**, 239–247 (1981).
51. Collawn, J.F. & Matalon, S. CFTR and lung homeostasis. *Am. J. Physiol. Lung Cell. Mol. Physiol.* **307**, L917–L923 (2014).
52. Yuk, J.M. & Jo, E.K. Crosstalk between autophagy and inflammasomes. *Mol. Cells* **36**, 393–399 (2013).
53. Soares, M.P., Gozzelino, R. & Weis, S. Tissue damage control in disease tolerance. *Trends Immunol.* **35**, 483–494 (2014).
54. Darrah, R.J. *et al.* Early pulmonary disease manifestations in cystic fibrosis mice. *J. Cyst. Fibros.* **15**, 736–744 (2016).
55. van der Doef, H.P. *et al.* Association of the CLCA1 p.S357N variant with meconium ileus in European patients with cystic fibrosis. *J. Pediatr. Gastroenterol. Nutr.* **50**, 347–349 (2010).
56. Young, F.D. *et al.* Amelioration of cystic fibrosis intestinal mucous disease in mice by restoration of mCLCA3. *Gastroenterology* **133**, 1928–1937 (2007).
57. Clarke, L.L. *et al.* Relationship of a non-cystic fibrosis transmembrane conductance regulator-mediated chloride conductance to organ-level disease in *Cfr*<sup>-/-</sup> mice. *Proc. Natl. Acad. Sci. USA* **91**, 479–483 (1994).
58. Boyle, M.P. *et al.* A CFTR corrector (lumacaftor) and a CFTR potentiator (ivacaftor) for treatment of patients with cystic fibrosis who have a Phe508del CFTR mutation: a phase 2 randomised controlled trial. *Lancet Respir. Med.* **2**, 527–538 (2014).
59. Fajac, I. & De Boeck, K. New horizons for cystic fibrosis treatment. *Pharmacol. Ther.* **170**, 205–211 (2017).
60. Pilewski, J.M., Donaldson, S.H., Cooke, J. & Lekstrom-Himes, J. Phase 2 studies reveal additive effects of VX-661, an investigational CFTR corrector, and ivacaftor, a CFTR potentiator, in patients who carry the  $\Delta F508$ -CFTR mutation. *Pediatr. Pulmonol.* **49**, 157–159 (2014).

## COMPETING FINANCIAL INTERESTS

A patent application by L.R. and E.G. is pending (filing date, 9 February 2016, RM2015A000056 and 102015000053089).

## EDITORIAL SUMMARY

**AOP:** Thymosin  $\alpha 1$  is used in the clinic as a treatment in viral disease and acts as an anti-inflammatory. Here it was found to also correct the misfolding of mutant CFTR and potentiate its activity, thus improving outcome in a mouse model of cystic fibrosis.

## ONLINE METHODS

**General experimental approaches.** Sample size was chosen empirically based on our previous experiences in the calculation of experimental variability; no statistical method was used to predetermine sample size and no samples, mice or data points were excluded from the reported analyses. Experimental groups were balanced in terms of animal age, sex and weight. No blinding was applied upon harvesting samples after the treatments.

**Mice.** Mouse experiments were performed according to Italian Approved Animal Welfare Authorization 360/2015-PR and Legislative Decree 26/2014 regarding the animal license obtained by the Italian Ministry of Health lasting for 5 years (2015–2020). Infections were performed under isoflurane anesthesia, and all efforts were made to minimize suffering. CF mice homozygous for the Phe508del-CFTR allele, which had been backcrossed for 12 generations to the C57BL/6 strain or on the FVB/129 outbred background (*Cftr*<sup>tm1IEUR</sup>, Phe508del, abbreviated *Cftr*<sup>F508del/F508del</sup>), were obtained from B. Scholte (Erasmus Medical Center)<sup>61</sup>. *Cftr*<sup>F508del/+</sup> female mice were backcrossed to C57BL/6-background *Becn1*<sup>+/-</sup> male mice to obtain *Becn1*-haploinsufficient F508del-homozygous mice (abbreviated *Cftr*<sup>F508del/F508del/Becn1</sup><sup>+/-</sup>), as described<sup>9</sup>. These mice were provided with a special food consisting of an equal mixture of SRM-A (Arie Blok, Woerden, The Netherlands) and Teklad 2019 (Harlan Laboratories, San Pietro al Natisone, Udine, Italy) and water acidified to pH 2.0 with HCl and containing 60g/l PEG 3350, 1.46g/l NaCl, 0.745g/l KCl, 1.68g/l NaHCO<sub>3</sub> and 5.68g/l Na<sub>2</sub>SO<sub>4</sub>. Newborn mice were genotyped by cutting a small piece of tail 12 d after birth. C57BL/6 mice aged 4–6 weeks purchased from Charles River (Calco, Italy) and genetically engineered homozygote knockout *Cftr* mice (B6.129P2-KO *Cftr*<sup>tm1UNC</sup>, abbreviated *Cftr*<sup>-/-</sup> and *Cftr*<sup>+/-</sup>, gut corrected, on a C57BL/6 background) were bred under specific-pathogen-free conditions at the Animal Facility of San Raffaele Hospital, Milan, Italy. Male and female mice were used in all studies.

**Infections and treatments.** Mice were anesthetized in a plastic cage by inhalation of 3% isoflurane (Forane, Abbott) in oxygen before intranasal instillation of  $2 \times 10^7$  *A. fumigatus* (Af293) resting conidia per 20  $\mu$ l of saline. For *P. aeruginosa* infection, appropriate dilutions with sterile PBS were made to prepare the inoculum before intranasal instillation of  $3 \times 10^7$  CFU per mouse<sup>22</sup>. Quantification of microbial growth was done as described<sup>22</sup>. For histology, paraffin-embedded sections were stained with periodic acid–Schiff (PAS) and H&E. Mice were treated either intraperitoneally (i.p.) or intranasally (i.n.) with T $\alpha$ 1 or the scrambled polypeptide reconstituted in sterile water (200  $\mu$ g per kg bodyweight in 20  $\mu$ l of saline (i.n.) or 100  $\mu$ l of saline (i.p.)) given daily for six consecutive days in uninfected mice either beginning the day of the infection or starting 7 d after the infection. Mice were weighed on the first and last days of the treatment. Mice were gavaged with cysteamine (60  $\mu$ g per kg bodyweight in 100  $\mu$ l of saline per day) for 6 d as reported<sup>62</sup>. For BAL fluid collection, lungs were filled thoroughly with 1-ml aliquots of pyrogen-free saline through a 22-gauge bead-tipped feeding needle introduced into the trachea. BAL fluid was collected in a plastic tube on ice and centrifuged at 400g at 4 °C for 5 min. For differential BAL fluid cell counts, cytospin preparations were made and stained with May–Grünwald Giemsa reagents (Sigma-Aldrich). At least 200 cells per field per 10 fields were counted, and the absolute number of neutrophils was calculated. For epithelial cell purification, lung epithelial cells, of which 99% expressed cytokeratin on pan-cytokeratin antibody staining of cytocentrifuge preparations and >90% were viable on trypan blue exclusion assay, were isolated as described<sup>63</sup>. Cells were stimulated with MALP-2, poly(I:C), ultrapure lipopolysaccharide from *Salmonella minnesota* Re 595 (all from Sigma-Aldrich) and CpG ODNs (all at 10  $\mu$ g/ml) for 1 h (NF- $\kappa$ B and IRF3 protein expression) or 4 h (*IL10* gene expression). Uncropped immunoblots are shown in the **Supplementary Data**.

**Cells.** HBE cells, homozygous for the p.Phe508del mutation, and isogenic wild-type cells were obtained from lung transplants (individuals with CF) or lung resections (controls) (kindly provided by L.J. Galletta, Italian Cystic Fibrosis Foundation). Cells were maintained at 37 °C in a humidified incubator in an atmosphere containing 5% CO<sub>2</sub>, and the experiments were done 5 d after plating<sup>64</sup>. Stable lentiviral-based transduction of the parental CFBE41o-cells, homozygous for the p.Phe508del-CFTR mutation<sup>24</sup>, with either WT CFTR or

p.Phe508del-CFTR were provided by L.J. Galletta. The transduced CFBE41o-cells were maintained in minimum Eagle's medium supplemented with 50 U/ml penicillin, 50  $\mu$ g/ml streptomycin, 2 mM L-glutamine, 10% FBS and 1  $\mu$ g/ml blasticidin (WT CFTR) or 2  $\mu$ g/ml puromycin (p.Phe508del-CFTR) in a 5% CO<sub>2</sub> and 95% air incubator at 37 °C. To establish polarized monolayers, CFBE41o-cells were seeded on 24-mm-diameter Transwell permeable supports (0.4- $\mu$ m pore size; Corning Corp., Corning, NY) at  $2 \times 10^6$  cells/well and grown in an air-liquid interface culture at 37 °C for 6–9 d and then at 27 °C for 36 h. Cells were incubated with different concentrations of T $\alpha$ 1 (CRIBI Biotechnology), 3  $\mu$ M VX-809 (Lumacaftor, Aurogene), 1  $\mu$ M VX-770 (Ivacaftor, Aurogene) alone or in combination for up to 24 h before the assessment of CFTR protein expression and function at either 37 °C or 26 °C. For washout experiments, after the treatment period, the medium was replaced with complete medium for the indicated time. DMSO vehicle alone (0.1%) was used as a control. T $\alpha$ 1 and the scrambled polypeptide were supplied as purified (the endotoxin levels were <0.03 pg/ml by a standard limulus lysate assay), sterile, lyophilized, acetylated polypeptide. The sequences were as follows: Ac-SDAAVDTSSEITTTDLKEKK EVVEEAEN-O (T $\alpha$ 1) (SEQ ID 1) and Ac-AKSDVKAETSSEIDTTLEDEKV EVKANE-OH (scrambled peptide) (SEQ ID 2). For cell cultures, CFBE41o-cells were stimulated with CpG ODN (10  $\mu$ g/ml) or MALP-2 (100 ng/ml) with or without 100 ng/ml of T $\alpha$ 1 for 2 h and then lysed for immunoblotting or assessed for cytokine analysis by RT-PCR. Recombinant IFN- $\gamma$ , from Santa Cruz Biotechnology, was used at the concentration of 10 ng/ml. HEK293 cells were maintained in DMEM supplemented with 50 U/ml penicillin, 50  $\mu$ g/ml streptomycin, 2 mM L-glutamine and 10% FBS in a 5% CO<sub>2</sub>, 95% air incubator at 37 °C. Regular testing for mycoplasma contamination was carried out by PCR. Human studies approval was obtained from institutional review boards at each site, and written informed consent was obtained from the participants or, in case of minors, from parents or guardian.

**Immunofluorescence and immunohistochemistry.** CFBE41o-cells were treated with 100 ng/ml T $\alpha$ 1 at 37 °C for 24 h, fixed in 2% formaldehyde for 15 min at room temperature and permeabilized in blocking buffer containing 5% FBS, 3% BSA and 0.5% Triton X-100 in PBS. The cells were then incubated at 4 °C with the primary antibody anti-CFTR (clone CF3, Abcam). After extensive washing with PBS, the slides were then incubated at room temperature for 60 min with goat anti-mouse antibody to CFTR followed by Alexa Fluor 555 (Clone Poly4053, BioLegend) and Alexa Fluor 488 anti-phalloidin (A12379, Thermo Fisher) for F-actin labeling. For intracellular routing, cells were plated in complete medium into chambered coverglass (Lab-Tek/Nunc; Thermo Scientific) in a temperature-regulated environmental chamber and exposed to 100 ng/ml T $\alpha$ 1 at 37 °C for 2 h in serum-free RPMI-1640 medium. After washout, cells were fixed, permeabilized and incubated at 4 °C with anti-Rab5, anti-Rab7, anti-Rab9 (all from Sigma) and anti-USP36 (clone 7G3, Abcam) primary antibodies. After extensive washing with PBS, the cells were incubated at room temperature for 60 min with a 1:400 dilution of FITC-conjugated anti-rabbit IgG secondary antibody (Sigma-Aldrich). For TLR9 colocalization, HEK293 cells that were transfected with human TLR9 tagged at its C terminus with enhanced GFP (TLR9-GFP) were obtained from G. Teti (University of Messina). Cells were seeded onto a sterilized coverslip, placed in a six-well plate and stimulated with 1  $\mu$ g/ml CpG ODN in the presence of 100 ng/ml T $\alpha$ 1 for 30 min. Cells were then fixed with 4% paraformaldehyde, permeabilized by 0.1% Triton X-100 and stained with biotin-conjugated anti-human CD107a antibody (BioLegend) for the LAMP-1 or with biotin-conjugated anti-transferrin receptor antibody (DF1513, Abcam) and visualized with streptavidin, Alexa Fluor 568 conjugate (Thermo Fisher). The tissues were removed and fixed in 10% phosphate-buffered formalin, embedded in paraffin and sectioned at 5  $\mu$ m. Sections were then rehydrated, and after antigen retrieval in citrate buffer (10mM, pH 6.0), sections were fixed in 2% formaldehyde for 40min at room temperature and permeabilized in blocking buffer containing 5% FBS, 3% BSA and 0.5% Triton X-100 in PBS. The sections were incubated at 4 °C overnight with anti-NLRP3 (ab4287, Abcam) primary antibody and then incubated at room temperature for 60min with Alexa Fluor 555-conjugated goat anti-mouse secondary antibody (Poly4053, BioLegend). For immunohistochemistry, sections were incubated overnight with anti-CFTR (CF3, Novus) or anti-CLCA1 (Abcam) antibody followed by biotinylated secondary antibodies. Cells were counterstained with

hematoxylin or DAPI to detect nuclei. All images were acquired using a BX51 fluorescence microscope (Olympus) with  $\times 20$ ,  $\times 40$  and  $\times 100$  objectives using the analysis image-processing software (Olympus).

**Western blot analysis and immunoprecipitation.** Blots of cell lysates were incubated with antibodies against the following proteins: CFTR (CF3, Abcam; CF3, Novus; 2269, Cell Signaling), CLCA1 (Abcam), USP36 (Proteintech), murine IDO1 (monoclonal; cv152)<sup>65</sup>, human IDO1 (10.1, Millipore), phospho-NF- $\kappa$ B/p65 and NF- $\kappa$ B/p65 (Cell Signaling), phospho-IRF3 (Cell Signaling) and IRF3 (Santa Cruz). For immunoprecipitation, cells were lysed in immunoprecipitation buffer containing 150 mM sodium chloride, 50 mM Tris (pH 8.0), 1% Triton X-100, 0.5% sodium deoxycholate, 0.1% SDS, Complete protease inhibitor cocktail (Roche) and PMSF (Roche). CFTR and IDO1 were immunoprecipitated by incubation with 1  $\mu$ g of the specific antibody. The reaction was performed overnight, and either Protein A (for CFTR) or Protein G (IDO1) Sepharose 4 Fast Flow beads (GE Healthcare) were added and incubated for an additional 2 h. Beads were washed and resuspended in Laemmli buffer. Immunoprecipitated proteins were separated by SDS-PAGE, and immunoblots were probed with anti-USP36, anti-Hsp70, anti-Hsp90 and anti-calnexin antibodies and with anti-ubiquitin antibody that recognizes mono-, oligo- or polyubiquitinated additions (all from Abcam). For physical association of T $\alpha$ 1 to CFTR, immunoprecipitated proteins were separated by tricine-SDS-PAGE<sup>66</sup>, and immunoblots were probed with anti-T $\alpha$ 1 antibody (ab76557, Abcam). Normalization was performed probing the membrane with  $\beta$ -actin or  $\beta$ -tubulin antibody (AC-15 or TUB 2.1, Sigma). Alternatively, lysates from HEK293 cells transfected with FLAG-T $\alpha$ 1 were immunoprecipitated using an affinity resin with anti-FLAG M2 (clone M2, Sigma) and the resulting FLAG-T $\alpha$ 1 resin was incubated in the presence of lysates from CFBE41o- cells transfected with WT CFTR or p.Phe508del-CFTR. Samples were resolved by immunoblotting and probed with anti-CFTR antibody. Lysates from p.Phe508del-CFTR CFBE41o- cells were transfected with FLAG-T $\alpha$ 1 and immunoprecipitated using the affinity resin with anti-FLAG M2. In order to avoid nonspecific binding, after elution with FLAG peptide (Sigma), the remaining proteins bound to the resin were loaded as a negative control. Samples were resolved by immunoblotting and probed with anti-CFTR antibody. Chemiluminescence detection was performed with LiteAbloPlus chemiluminescence substrate (Buroclone), using the ChemiDoc XRS + Imaging system (Bio-Rad), and quantification was obtained by densitometry image analysis using Image Lab 5.1 software (Bio-Rad). Uncropped immunoblots are shown in the **Supplementary Data**.

**Luciferase assays.** CFBE41o- cells were seeded in 24-well plates at a density of  $7.5 \times 10^4$  cells per well. Cells were transfected using Lipofectamine 2000 (Invitrogen) according to the manufacturer's protocol. Each transfection contained 100 ng of a luciferase reporter plasmid (pLV-5X-NF- $\kappa$ B-RE Luc) and 50 ng of a  $\beta$ -galactosidase internal-control reporter plasmid (pGL3-lacZ) with or without MALP-2 (100 ng/ml). The total amount of DNA applied per well was adjusted to 600 ng by adding pcDNA3 empty vector. Cell extracts were subjected to a luminometry-based luciferase assay, and luciferase activity was normalized by  $\beta$ -galactosidase activity.

**Membrane fractionation.** Cells were homogenized with a Potter-Elvehjem pestle and centrifuged at 2,300g for 15 min at 4 °C. Supernatant fractions that contained the cytoplasmic and plasma membrane fractions were centrifuged 1 h at 16,000g at 4 °C; the pellet was the intact membrane and was solubilized in buffer A (20 mM Tris-HCl, pH 7.4, 2 mM EDTA, 20 mM 2-mercaptoethanol, 1 $\times$  PMSF, 1 mg/ml protease inhibitor cocktail (P8340, Sigma), 0.1% Triton X-100 (X-100-RS, Sigma)) and centrifuged 1 h at 60,000g in the ultracentrifuge. The supernatant fractions were collected as a plasma membrane fraction, proteins were separated by SDS-PAGE and immunoblots were probed with anti-CFTR (Cell Signaling) and anti-flotillin 1 (Sigma) antibodies. Uncropped immunoblots are shown in the **Supplementary Data**.

**CFTR half-life.** Cycloheximide (40  $\mu$ g/ml) was added to CFBE41o- cells treated with 100 ng/ml T $\alpha$ 1 for 24 h at 37 °C for up to 6 h. Cell lysates were assessed for CFTR protein expression by western blotting. Uncropped immunoblots are shown in the **Supplementary Data**.

**Proteasome and lysosome assays.** CFBE41o- cells were plated in a 12-well cell culture plate and stimulated with T $\alpha$ 1 (100 ng/ml) for 2 h at 37 °C. For proteasome activity, cells were lysed with NP-40 lysis buffer and the amount of picomoles of proteolytic activity was analyzed with the proteasome activity assay kit (Abcam) that takes advantage of chymotrypsin-like activity, using an AMC-tagged peptide substrate (Succ-LLVY-AMC), which releases free, highly fluorescent AMC in the presence of proteolytic activity. For lysosomal activity, the Lysosome/Cytotoxicity Dual-Staining kit (Abcam) was used per the manufacturer's instructions.

**Limited proteolysis of CFTR.** CFBE41o- cells were treated for 2 h at 37 °C and lysed in PBS with Triton X-100 (0.1%) for 1 h at 4 °C. Lysates were cleared by centrifugation at 20,000 rpm for 10 min in a Beckman Allegra 64R centrifuge. Supernatants were removed, and total protein was determined by Quant-iT Protein Assay kit (Thermo Scientific) following the manufacturer's instructions. Cell lysates were then diluted to a concentration of 20  $\mu$ g/ml, and trypsin was added at the indicated final concentrations. The cleavage reactions were incubated on ice for 15 min and were then quenched by addition of complete protease inhibitor (Roche) and trypsin inhibitor. Sample buffer was added to a final 1 $\times$  concentration, and samples were run on 7% SDS-PAGE gels. Uncropped immunoblots are shown in the **Supplementary Data**.

**Identification of active deubiquitinases.** CFBE41o- cells were lysed in immunoprecipitation assay buffer (25 mM Tris-HCl, pH 7.6, 10 mM NaCl, 1% Triton X-100, 1% sodium deoxycholate, 0.1% SDS), and 0.1  $\mu$ g of the HA-Ub-VME probe (Enzo) was added to 20  $\mu$ g of protein extract. HA-Ub-VME probe forms an irreversible covalent bond with active DUBs. Identification of DUBs covalently linked to the HA-Ub-VME probe was achieved by immunoprecipitation of HA-Ub-VME-DUB complexes using an anti-HA antibody (A190-108A, Bethyl Laboratories) followed by SDS-PAGE and western blot analysis using anti-DUB antibodies specific to USP19 (Bethyl Laboratories), USP10 (Bethyl Laboratories) and USP36 (Proteintech). The specificity of the HA-Ub-VME probe for active DUBs was confirmed with the addition of *N*-ethylmaleimide (10  $\mu$ M) to inhibit cysteine protease DUBs during the labeling reaction. Uncropped immunoblots are shown in **Supplementary Data**.

**Plasmids and transfection.** The FLAG-HA-USP36 plasmid was a gift from W. Harper (Addgene plasmid 23679)<sup>67</sup> and was used for transfection experiments. For generation of the plasmid encoding pcDNA3.1/myc-His with the prothymosin  $\alpha$  (PTMA) fragment, the coding sequence of PTMA cDNA was amplified by PCR with specific primers containing EcoRI and XhoI anchor sites. The fragment was then subcloned into the EcoRI and XhoI cloning sites of the pcDNA3.1/myc-His A plasmid (Thermo Fisher Scientific) to construct the recombinant pcDNA3.1/myc-His-PTMA expression vector. To isolate the sequence encoding the T $\alpha$ 1 active peptide, the cDNA sequence corresponding to T $\alpha$ 1 was amplified by PCR with specific primers containing EcoRI and XhoI anchor sites, using PTMA pcDNA3.1/myc-His A as a template, and was cloned into the pCMV-Tag 2B expression vector (Agilent Technologies). Transient transfections were performed with a pCMV vector expressing FLAG-T $\alpha$ 1 using TransIT Transfection Reagent (Mirus), according to the manufacturer's instructions, in HEK293 cells and HBE Phe508del cells incubated for 24 h at 37 °C in 5% CO<sub>2</sub>. The empty vector was used as a negative control.

**RNA interference.** Pooled duplexes of predesigned siRNA (USP36, MMC.RNAI.N007887.12.1; CLCA1, MMC.RNAI.N001285.12.1) were purchased from IDT (TEMA Ricerca). Specific siRNA for prothymosin  $\alpha$  was purchased from Sigma. For siRNA delivery, cells were incubated for 24 h (as indicated by preliminary experiments performed at 12, 24 or 48 h) at 37 °C in 5% CO<sub>2</sub> with specific siRNA using TransIT-TKO Transfection Reagent (Mirus) following the manufacturer's instructions. The effectiveness of the silencing of specific targets was verified by evaluating target mRNA levels using RT-PCR (**Supplementary Fig. 8d**), and protein expression was evaluated by western blotting (**Figs. 3g and 6g**).

**Autophagy.** RAW 264.7 cells (ATCC) were seeded in 100-mm Petri dishes ( $3.5 \times 10^6$  cells/plate) and transfected with EGFP-LC3 plasmid (Addgene) using ExGen 500 *In Vitro* Transfection Reagent (Fermentas) for 48 h, according to the

manufacturer's instructions. Transiently transfected RAW 264.7 cells or HBE cells from patients with CF harboring the p.Phe508del mutation were exposed to 1 or 100 ng/ml T $\alpha$ 1 for 4 h at 37 °C in 5% CO $_2$ , as described<sup>68</sup>. Cultures growing on coverslips were observed at  $\times$ 100 magnification with the Olympus BX51 fluorescence microscope using a FITC filter. Results are expressed as the number of cells with EGFP-LC3 puncta. An equal amount of cell lysate in 2 $\times$  Laemmli buffer (Sigma) was probed with HRP-conjugated rabbit anti-LC3B (Cell Signaling) and goat anti-rabbit (Sigma) secondary antibody or with anti- $\beta$ -actin-1 (Cell Signaling) and anti-SQSTM1/p62 (Cell Signaling) antibodies. Normalization was performed by probing the membrane with anti- $\beta$ -tubulin antibody (Sigma). Alveolar macrophages from C57BL/6 and *Indo*<sup>-/-</sup> lung cells were isolated after 2 h of plastic adherence at 37 °C and treated with T $\alpha$ 1 as described above before assessment of LC3 expression by immunofluorescence. Chemiluminescence detection was performed with LiteAblot Plus chemiluminescence substrate (EuroClone), using the ChemiDoc XRS+ imaging system (Bio-Rad), and quantification was obtained by densitometry image analysis using Image Lab 5.1 software (Bio-Rad). Uncropped immunoblots are shown in the **Supplementary Data**.

**Functional analysis of CFTR and calcium-activated chloride currents.** Patch-clamp recordings were performed from p.Phe508del-CFTR-transfected CFBE41o- cells (treated with 100 ng/ml T $\alpha$ 1 for 2 or 24 h at 37 °C) and from bronchial epithelial cells derived from *Cfr*<sup>P508del</sup> C57BL/6 mice. CFTR single-channel activity was measured at 25 °C by means of the on-cell configuration, using an Axopatch 200B amplifier (Axon Instruments). Both the pipette and bath solutions contained 140 mM *N*-methyl-D-glucamine, 5 mM CaCl $_2$ , 2 mM MgSO $_4$  and 10 mM TES (adjusted to pH 7.30 with HCl), total [Cl $^-$ ] $_o$  = 140 mM. Seal resistances ranging from 5 to 20 G $\Omega$  were obtained. The membrane potential was maintained at -40 mV, and pulses from -100 to +100 mV, each lasting 5 s, were delivered. Pipettes with a resistance of 5–10 M $\Omega$  were pulled from borosilicate glass capillary tubing (GC150-F10, Clark Electromedical) using a two-step horizontal puller from Sutter Instrument. Cells were stimulated with forskolin (Fsk; 10  $\mu$ M) and genisteine (Gen; 30  $\mu$ M). Single-channel recordings were sampled at 5 kHz and filtered at 200 Hz with an eight-pole Bessel filter. Macroscopic CFTR and calcium-activated chloride currents were recorded by means of the whole-cell configuration, using an EPC 10-patch-clamp amplifier (HEKA Elektronik). Current-voltage (*I*-*V*) relationships were built by clamping the membrane potential of CFBE41o- cells at -40 mV and by delivering ramps from -100 mV to +50 mV. The pipette solution contained 113 mM L-aspartic acid, 113 mM CsOH, 27 mM CsCl, 1 mM NaCl, 1 mM MgCl $_2$ , 1 mM EGTA and 10 mM TES (pH 7.2). MgATP (3 mM) was added just before the patch-clamp experiments were started. The external solution contained 145 mM NaCl, 4 mM CsCl, 1 mM CaCl $_2$ , 10 mM glucose and 10 mM TES (pH 7.4). Results were analyzed with PATCHMASTER software (HEKA Elektronik).

The colorimetric assay with SPQ (6-methoxy-*N*-(3-sulfo-propyl) quinolinium) fluorescent probe (Molecular Probes/Invitrogen)<sup>69</sup> was also used to estimate CFTR channel activity. Briefly, the iodide-sensitive fluorescent indicator SPQ was introduced into the cells in a hypotonic solution of iodide buffer (130 mM NaI, 4 mM KNO $_3$ , 1 mM Ca(NO $_3$ ) $_2$ , 1 mM Mg(NO $_3$ ) $_2$  (all from Sigma-Aldrich), 10 mM glucose and 20 mM HEPES, pH 7.4) diluted 1:1 with water and containing a final concentration of 10 mM SPQ. Cells were loaded for 20 min at 37 °C in a humidified chamber with 5% CO $_2$ . The SPQ-loaded cells were assessed with the TECAN plate reader (Thermo Fisher Scientific) with a 37 °C heated stage and perfused with iodide buffer for 5–8 min. Changes in CFTR-mediated SPQ fluorescence were monitored at 445 nm in response to excitation at 340 nm during perfusion at 37 °C in nitrate buffer replaced with 130 mM NaNO $_3$  with 20  $\mu$ M forskolin plus 100  $\mu$ M IBMX (all from Sigma-Aldrich) and fluorescence intensity measured for a further 10–12 min. Signals were collected at 30-s intervals. For each minute, the average of the fluorescence intensity was measured from 50 cells for population per coverslip and the peak of the iodide efflux rate (usually after addition of Fsk plus IBMX) of cells was calculated in accordance with the Stern-Volmer relationship as follows:  $(F_0/F) - 1 = K_C Q$ , where *F* is the observed fluorescence, *F* $_0$  is the fluorescence in the absence of a quenching anion, *C* $_Q$  is the concentration of the quenching anion and *K* is the Stern-Volmer quench constant.

**Preparation of RNA and microarray hybridization.** Total-lung RNA was extracted using TRIzol reagent (Life Technologies). The integrity of total RNA was evaluated using the Agilent Bioanalyzer 2100 system (Agilent Technologies) and was within RNA integrity number 7–9 and thus considered suitable for further processing. 100 ng of total RNA was processed to produce fragmented biotin-labeled cDNA using the GeneChip WT PLUS Reagent kit according to the manufacturer's instructions. Samples were hybridized to Affymetrix GeneChip Mouse Gene 2.0 ST arrays and quantified. Images were processed and cell intensity files (CEL files) were generated in GeneChip Command Console Software (Affymetrix). CEL files were processed using Expression Console v.1.4.1.46 to yield RMA-summarized log $_2$ -transformed expression values for probe sets (CHP files). Normalized expression data (CHP files) were analyzed using Transcriptome Analysis Console Software (Affymetrix) and ANOVA in R using the Bioconductor R package.

**Using chamber.** Chambers for mounting tissue biopsy were obtained from Physiologic Instruments (model P2300). Chamber solution was buffered by bubbling with a mixture of 95% O $_2$  and 5% CO $_2$ . Tissues were short-circuited using Ag/AgCl agar electrodes. Short-circuit current and resistance were acquired or calculated using the VCC-600 transepithelial clamp from Physiologic Instruments and Acquire & Analyze 2.3 software for data acquisition (Physiologic Instruments), as previously described<sup>9</sup>. A basolateral-to-apical chloride gradient was established by replacing NaCl with sodium gluconate in the apical (luminal) compartment to create a driving force for CFTR-dependent Cl $^-$  secretion. CFTR channels present at the apical surface of the epithelium (lumen side of the tissue) were activated. Stimulations with forskolin, CFTR inhibitor 172 and amiloride were performed as described<sup>9</sup>.

**ELISA and real-time PCR.** The levels of cytokines were determined by specific ELISAs (R&D Systems). For T $\alpha$ 1 production (ELISA kit from Immundiagnostik), either cell culture supernatants or cell lysates were used. RT-PCR was performed using the Bio-Rad CFX96 System and SYBR Green chemistry (Bio-Rad). The PCR primers were as follows: *IL10* Forward, 5'-GCCTAACATGCTTCGAGATC-3' and Reverse, 5'-TGATGTCTGGTCTTGGTTC-3'; *IL6* Forward, 5'-CCACTCACCTCTTCAGAAGCAATT-3' and Reverse, 5'-AGTGCCTCTTTCGCTTTCA-3'; *CLCA1* Forward, 5'-GCTGATGTTCTGGTTGCTGA-3' and Reverse, 5'-CGTCAAATACTCCCATCGT-3'; *Clcn1* Forward, 5'-AGCCA GGAGCCTCGCCCGCAGCTGCA-3' and Reverse, 5'-CGGGTTGCCT GCAAAGT-3'; *Clea3* Forward, 5'-AAACGAGAAGGCTTCCATCA-3' and Reverse, 5'-GGAGATTGCATCGTTGGTTT-3'. Amplification efficiencies were validated and normalized against *ACTB*. Each data point was examined for integrity by analysis of the amplification plot. The mRNA-normalized data were expressed as relative gene mRNA in treated as compared to untreated experimental groups or cells.

**Statistical analysis.** GraphPad Prism software 6.01 (GraphPad Software) was used for analysis. Data are expressed as means  $\pm$  s.d. Horizontal bars indicate the means. Plots of *in vivo* data are presented as box-and-whiskers plots; bars represent maximal and minimal values. Statistical significance was calculated by one- or two-way ANOVA (Tukey's or Bonferroni's *post hoc* test) for multiple comparisons and by a two-tailed Student's *t*-test for single comparisons. The distribution of levels tested by the Kolmogorov-Smirnov normality test turned out to be non-significant. The variance was similar in the groups being compared. We considered all *P* values 0.05 to be significant. The *in vivo* groups consisted of six mice/group. The data reported are either representative of at least three experiments (histology, immunofluorescence and western blotting) or pooled otherwise.

**Data availability.** The data that support the findings of this study are available from the corresponding author upon reasonable request.

61. van Doorninck, J.H. *et al.* A mouse model for the cystic fibrosis  $\Delta$ F508 mutation. *EMBO J.* 14, 4403–4411 (1995).

62. De Stefano, D. *et al.* Restoration of CFTR function in patients with cystic fibrosis carrying the F508del-CFTR mutation. *Autophagy* 10, 2053–2074 (2014).

63. de Luca, A. *et al.* Non-hematopoietic cells contribute to protective tolerance to *Aspergillus fumigatus* via a TRIF pathway converging on IDO. *Cell. Mol. Immunol.* **7**, 459–470 (2010).
64. Loffing, J., Moyer, B.D., McCoy, D. & Stanton, B.A. Exocytosis is not involved in activation of Cl<sup>-</sup> secretion via CFTR in Calu-3 airway epithelial cells. *Am. J. Physiol.* **275**, C913–C920 (1998).
65. Pallotta, M.T. *et al.* Indoleamine 2,3-dioxygenase is a signaling protein in long-term tolerance by dendritic cells. *Nat. Immunol.* **12**, 870–878 (2011).
66. Schägger, H. Tricine-SDS-PAGE. *Nat. Protoc.* **1**, 16–22 (2006).
67. Sowa, M.E., Bennett, E.J., Gygi, S.P. & Harper, J.W. Defining the human deubiquitinating enzyme interaction landscape. *Cell* **138**, 389–403 (2009).
68. De Luca, A. *et al.* CD4<sup>+</sup> T cell vaccination overcomes defective cross-presentation of fungal antigens in a mouse model of chronic granulomatous disease. *J. Clin. Invest.* **122**, 1816–1831 (2012).
69. Munkonge, F. *et al.* Measurement of halide efflux from cultured and primary airway epithelial cells using fluorescence indicators. *J. Cyst. Fibros.* **3** (Suppl. 2), 171–176 (2004).

Q116